

“FAULT DETECTION OF CRACKED CANTILEVER BEAM USING SMART TECHNIQUE”

A THESIS SUBMITTED IN PARTIAL FULFILLMENT OF
THE REQUIREMENTS FOR THE DEGREE OF

Master of Technology
in
Mechanical Engineering

[Specialization: Machine Design and Analysis]

By

MIHIR KUMAR SUTAR
207ME115

Under the supervision of
Dr. D.R.K. Parhi
Department of Mechanical Engineering, N.I.T. Rourkela



Department of Mechanical Engineering
**NATIONAL INSTITUTE OF TECHNOLOGY
ROURKELA**

MAY, 2009



National Institute of Technology

Rourkela

CERTIFICATE

This is to certify that the work in this project report entitled “**Fault Detection of Cracked Cantilever Beam using Smart Technique**” by **Mihir Kumar Sutar** has been carried out under my supervision in partial fulfillment of the requirements for the degree of **Master of Technology** in *Mechanical Engineering* with “**Machine Design and Analysis**” specialization during session 2008 - 2009 in the Department of Mechanical Engineering, National Institute of Technology, Rourkela.

To the best of our knowledge, this work has not been submitted to any other University/Institute for the award of any degree or diploma.

Date: 26/05/09

ROURKELA

Prof. D.R.K. Parhi
Professor,
Dept. of Mechanical Engineering
National Institute of Technology,
Rourkela – 769008, Orissa, INDIA

ACKNOWLEDGEMENT

Successful completion of work will never be one man's task. It requires hard work in right direction. There are many who have helped to make my experience as a student a rewarding one.

In particular, I express my gratitude and deep regards to my thesis guide **Prof.D.R.K. Parhi** for kindly providing me to work under his supervision and guidance. I extend my deep sense of indebtedness and gratitude to him first for his valuable guidance, constant encouragement & kind co-operation throughout period of work which has been instrumental in the success of thesis.

I also express my sincere gratitude to **Prof. R. K. Sahoo**, Head of the Department, Mechanical Engineering, for providing valuable departmental facilities.

I am greatly indebted to my family members for extending their loving support throughout.

I bow to the Devine power, who led me all through

Date: - 26/05/09

Mihir Kumar Sutar

Roll No: - 207ME115

M.Tech. (Machine Design and Analysis)

Department of Mechanical Engineering

NIT Rourkela, Orissa,

INDIA

Abstract

Over the years damage detection in structures is being given prior attention. For this purpose different newer techniques are being used so far. In this investigation defect in cantilever beam in the form of a transverse crack is being investigated using smart Technique like Fuzzy Logic. Gaussian membership functions are used for the Fuzzy Controller. The input parameters to the Fuzzy Controller are relative divergence of first three natural frequencies and the output parameters of the Fuzzy Controller are relative crack depth and relative crack location in dimensionless forms. For deriving the fuzzy rules for the controller; theoretical expressions have been developed considering three parameters such as; natural frequencies, crack depths and crack locations. Strain energy release rate has been used for calculating the local stiffnesses of the beam. The local stiffnesses of the beam are dependent on the crack depth. Different boundary conditions are being outlined which take into account the crack location. Several fuzzy rules are derived and the Fuzzy controller has been designed accordingly. Experimental setup has been developed for verifying the robustness of the developed fuzzy controller. Finite Element Analysis is performed on the single and double cracked cantilever beam to obtain the modal natural frequencies. The proposed approach is verified by comparing the results obtained from the numerical analysis and the developed experimental set-up. And it was observed that the Fuzzy Controller can predict the location and depth of the crack in a close proximity as par with the actual results.

CONTENTS

Name of the Content	Page
Certificate	i
Acknowledgement	ii
Abstract	iii
Contents	iv
List of Tables	vi
List of Figures	vii
Nomenclature	xi
Chapter 1: Introduction	1
1.1 Background	1
1.2 Aims and Objectives of this Research	4
1.3 Outline of the Thesis	5
Chapter 2: Literature Review	7
Chapter 3: Theoretical Analyses	26
3.1 Local flexibility of a Cracked Beam under Bending and Axial Loading.	26
3.2 Analysis of Vibration Characteristics of the Cracked Beam	30
3.2.1 Free Vibration	30
3.2.2 Forced Vibration	32
Chapter 4: Fuzzy Controller Analysis	34
4.1 Introduction	34
4.2 Fuzzy Set Theory	34
4.3 Membership Function	34
4.3.1. Membership functions in Fuzzy Logic- Tool Box	34
4.4. Linguistic Variables	36

4.5.	Fuzzy Rules	36
4.6.	Fuzzy Controller Analysis for the Crack Localization and Identification	37
4.7	Fuzzy mechanism used for crack detection	41
4.8	Output (Crack Length and crack Depth) using Fuzzy Controller	43
Chapter 5: Finite Element Formulation		46
5.1	Theory	46
5.2	Governing Equation of Free Vibration	46
5.3	Governing Equation of Forced Vibration	49
5.4	Simulated Crack configuration	51
5.5	Finite Element Modeling	57
Chapter 6: Results and Discussions		62
6.1	Experimental Set-up	62
6.2	Results	62
6.3	Discussions	75
Chapter 7: Conclusions		77
7.1	Scope for Future Work	77
References		78

List of Tables

Table	Title	Page
Table 4.1	Fuzzy Linguistic Terms used	40
Table 4.2	Example of some fuzzy rules used in the Fuzzy Controller	44
Table 6.1	Comparison of Results among Fuzzy Controller, Numerical Analysis and Experimental Analysis	75

List of Figures

Table	Title	Page
Fig. 3.1 (a)	Geometry of the Cracked Cantilever Beam	26
Fig. 3.1 (b)	Cross-sectional View of the Beam	27
Fig. 3.1 (c)	Segments taken during Integration at the Crack section	27
Fig. 3.2	Beam model	30
Fig. 4.1	Membership Functions shown in the Fuzzy Controller	37
Fig: 4.1 (a)	Membership functions for relative natural frequency for 1 st Mode of Vibration	38
Fig: 4.1 (b)	Membership functions for relative natural frequency for 2 nd Mode of Vibration	38
Fig: 4.1 (c)	Membership functions for relative natural frequency for 3 rd Mode of Vibration	38
Fig: 4.1 (d)	Membership functions for crack depth	39
Fig: 4.1 (e)	Membership functions for crack length	39
Fig. 4.2	Resultant values of relative crack depth and relative crack location when Rule 20 are activated	43
Fig. 4.3	Surface view of relative first and second natural frequency with relative crack depth	45
Fig. 4.4	Surface view of relative first and third natural frequency with relative crack length	45
Fig. 5.1	Crack location at $L_1 = 50$ mm and crack depth $a_1 = 0.202$	52
Fig. 5.2	Crack location at $L_1 = 100$ mm and crack depth $a_1 = 0.202$	52

Table	Title	Page
Fig. 5.3	Crack location at $L_1 = 200$ mm and crack depth $a_1 = 0.202$	53
Fig. 5.4	Crack location at $L_1 = 200$ mm and crack depth $a_1 = 0.202$	53
Fig. 5.5	Crack location at $L_1 = 300$ mm and crack depth $a_1 = 0.202$	54
Fig. 5.6	Crack location at $L_1 = 400$ mm and crack depth $a_1 = 0.202$	54
Fig. 5.7	Crack location at $L_1 = 500$ mm and crack depth $a_1 = 0.202$	55
Fig. 5.8	Crack location at $L_1 = 600$ mm and crack depth $a_1 = 0.202$	55
Fig. 5.9	Crack location at $L_1 = 700$ mm and crack depth $a_1 = 0.202$	56
Fig. 5.10	Two Crack location at $L_1 = 100$ mm and $L_2 = 700$ mm with crack depth $a_1 = 0.202$	56
Fig. 5.11	Finite Element modeling of the uncracked cantilever beam in ALGOR	58
Fig. 5.12	Finite Element modeling of the single-cracked cantilever beam in ALGOR	58
Fig. 5.13	Details of the crack zone in ALGOR environment	59
Fig. 5.14	Finite Element modeling of the double-cracked cantilever beam in ALGOR	59
Fig. 5.15 (a)	1 st mode frequency of the cracked cantilever beam model	60
Fig. 5.15 (b)	2 nd mode frequency of the cracked cantilever beam model	60
Fig. 5.15 (c)	3 rd mode frequency of the cracked cantilever beam model	61
Fig. 6.1	Schematic block diagram of Experimental Set-up	63

Table	Title	Page
Fig. 6.2	Experimental set-up	64
Fig. 6.3	INSTRON Set-up	65
Fig. 6.4	First Mode Natural Frequency versus crack depth	66
Fig. 6.5	Second Mode Natural frequency versus crack depth	66
Fig. 6.6	Third mode Natural Frequency versus crack depth	67
Fig. 6.7	Comparison of First Mode Natural Frequency at 50 mm and 100 mm	68
Fig. 6.8	Comparison of First Mode Natural Frequency at 50 mm and 200 mm	68
Fig. 6.9	Comparison of First Mode Natural Frequency at 50 mm and 300 mm	69
Fig. 6.10	Comparison of First Mode Natural Frequency at 50 mm and 400 mm	69
Fig. 6.11	Comparison of First Mode Natural Frequency at 50 mm and 500 mm	70
Fig. 6.12	Comparison of First Mode Natural Frequency at 50 mm and 600 mm	70
Fig. 6.13	Comparison of First Mode Natural Frequency at 50 mm and 700 mm	71
Fig. 6.14	Comparison of Second Mode Natural Frequency at 50 mm and 200 mm	71
Fig. 6.15	Comparison of Third Mode Natural Frequency at 50 mm and 300 mm	72
Figure 6.16	The change in First mode natural frequencies with crack location at 0.00833 relative Crack depth	72
Figure 6.17	The change in Second mode natural frequencies with crack location at 0.00833 relative Crack depth	73

Table	Title	Page
Figure 6.18	The change in Second mode natural frequencies with crack location at 0.00833 relative Crack depth	73
Figure 6.19	Three dimensional cum contour plot for relative First Mode Natural Frequency	74

Nomenclature

a_1	depth of crack
A	cross-sectional area of the beam
A_i	$i = 1$ to 12	unknown coefficients of matrix A
B	width of the beam
B_1	vector of exciting motion
C_u	$\left(\frac{E}{\rho}\right)^{1/2}$
C_y	$\left(\frac{EI}{\mu}\right)^{1/2}$
E	Young's modulus of elasticity of the beam material
f_{nf}	relative first natural frequency
F_i	$i = 1, 2$	experimentally determined function
i, j	variables
J	strain-energy release rate
$K_{1,i}$	$i = 1, 2$	stress intensity factors for P_i loads
\bar{K}_u	$\omega L / C_u$
\bar{K}_y	$\left(\frac{\omega L^2}{C_y}\right)^{1/2}$
K_{ij}	local flexibility matrix elements
L	length of the beam
L_1	location (length) of the crack from fixed end
M_i	$i=1,4$	compliance constant
P_i	$i=1,2$	axial force ($i=1$), bending moment ($i=2$)
Q	stiffness matrix for free vibration.
Q_1	stiffness matrix for forced vibration

rcd relative crack depth
 rcl relative crack location
 snf relative second natural frequency
 tnf relative third natural frequency
 u_i $i=1,2$ normal functions (longitudinal) $u_i(x)$
 x co-ordinate of the beam
 y co-ordinate of the beam
 Y_0 amplitude of the exciting vibration
 y_i $i=1,2$ normal functions (transverse) $y_i(x)$
 W depth of the beam
 ω natural circular frequency
 β relative crack location (L_1/L)
 μ $A X \rho$
 ρ mass-density of the beam
 ξ_1 relative crack depth (a_1/W)
 Λ minimum (min) operation
 \forall for every

Chapter 1

Introduction

1. Introduction

1.1 Background

Mechanical structures in real service life are subjected to combined or separate effects of the dynamic load, temperature and corrosive medium, due to the consequent growth of fatigue cracks, cracks due to corrosion and other type damages. The interest in the ability to monitor a structure and detect damage at the earliest possible stage is pervasive throughout the Civil, Mechanical and Aerospace Engineering communities. Damage is basically defined as changes introduced into a system, either intentional or unintentional, which adversely affect the current or future performance of that system. The immediate visual detection of damage is difficult or impossible in most of the cases and use of local non-destructive testing (NDT) methods of damage detection requires time and financial expense and is frequently inefficient. This has motivated the development of alternative methods. In this connection, the use of vibration-based methods of damage/crack diagnostics is promising. These methods are based on the vibration characteristics of structures such as natural frequencies and mode shapes. The vibration-based methods can help to determine the location and size of crack from the vibration signatures of the structures.

It is required that structures must safely work during its service life. But, damages initiate a breakdown period on the structures. Cracks are among the most encountered damage types in the structures. Cracks in a structure may be hazardous due to static or dynamic loadings, so that crack detection plays an important role for structural health monitoring applications.

It has been observed that the presence of cracks in structures or in machine members lead to operational problem as well as premature failure. A number of researchers throughout the world are working on structural dynamics and particularly on dynamic characteristics of structures with crack. Due to presence of cracks the dynamic characteristics of structure changes. These are the natural frequencies, the amplitude responses due to vibration and the mode shapes.

Cracks present a serious threat to proper performance of structures and machines. Most of the failures are due to material fatigue. For this reason methods allowing early detection and localization of cracks have been the subject of intensive research for investigations. Since the last two decades a number of experiments and theories have been developed to elucidate the phenomenon and determine the crack initiation and propagation conditions.

Beams are one of the most commonly used structural elements in numerous engineering applications and experience a wide variety of static and dynamic loads. Cracks may develop in beam-like structures due to such loads. Considering the crack as a significant form of such damage, its modelling is an important step in studying the behavior of damaged structures. Knowing the effect of crack on stiffness, the beam or shaft can be modeled using either Euler-Bernoulli or Timoshenko beam theories. The beam boundary conditions are used along with the crack compatibility relations to derive the characteristic equation relating the natural frequency, the crack depth and location with the other beam properties. As stated Beam type structures are being commonly used in steel construction and machinery industries. Studies based on structural health monitoring for crack detection deal with change in natural frequencies and mode shapes of the beam. The others deal with dynamic response of the beam due to harmonic forcing.

Fatigue cracks are a potential source of catastrophic structural failure. To avoid failure caused by cracks, many researchers have performed extensive investigations to develop structural integrity monitoring techniques. Most of these techniques are based on vibration measurements and analysis because, in most cases, vibration-based methods can offer an effective and convenient way to detect fatigue cracks. Generally, vibration-based methods can be classified into two categories: linear and nonlinear approaches. Linear approaches detect the presence of cracks in a target object by monitoring changes in the resonant frequencies in the mode shapes or in the damping factors. Depending on the assumptions, the type of analysis, the overall beam characteristics and the kind of loading or excitation, a huge number of publications containing a variety of different approaches have been reported in the relevant literature. In recent years, transport

engineering has experienced serious advances characterized mainly by parameters like higher speeds and weights of vehicles. These parameters make the transportation problem more complex.

With a race towards high speed, high power and lightweight in rotating machinery design and operation often impose severe stress and environmental condition upon rotors. As rotating machinery is designed to operate at higher mechanical efficiency; operating speed, power, and load are increased as weight and dimensional tolerances are decreased. High torsional and radial loads, together with a complex pattern of rotor motion, can create a severe mechanical stress condition that may eventually lead to development of a crack in the shaft. The presence of a transverse crack in shaft/rotor incurs a potential risk of destruction or collapse. This produces high costs of production and maintenance.

Detection of a crack in its early stages may save the rotor for use after repair. By monitoring, depending upon the type and severity of the crack, it may be possible in some cases to extend the use of a flawed rotor without risking a catastrophic failure, while arrangements are being made for a replacement rotor. The method will also improve safety by helping to prevent major rotor failure. For the time being, the research on cracked rotor is still at the theoretical stage.

With a well known fact the dynamic behavior of a structure with cracks is of significant importance in engineering. There are two types of problems related to this topic: the first may be called direct problem and the second called inverse problem. The direct problem is to determine the effect of damages on the structural dynamic characteristics, while the inverse problem is to detect, locate and quantify the extent of the damages. In the past two decades, both the direct and the inverse problems have attracted many researchers.

A direct procedure is difficult for crack identification and unsuitable in some particular cases, since they require minutely detailed periodic inspections, which are very costly. In order to avoid these costs, recently researchers have adopted an alternative and more efficient procedure in crack detection through vibration analysis.

1.2 Aims and Objectives of this Research

In the present investigation, a number of papers published so far have been surveyed, reviewed and analyzed. Most of the researchers studied the effect of a single crack on the dynamics of structures. However, in actual practice structural members such as beams/shafts are highly susceptible to transverse cross-sectional cracks due to fatigue. Some information is available on dynamics of structures due to crack but this is not exhaustive for real applications. Therefore an attempt has been made to formulate a Smart Technique for localization and identification of crack in cantilever beam structures. In the analysis both single and double cracks are taken into account.

The phases of the process plan for the present investigation are as follows;

1. Theoretical free and forced Vibration analysis of the single and double cracked cantilever beam.
2. Experimental Analysis to obtain the Relative values of first, second and third modal natural frequencies.
3. To train the series of data obtained in the experimental analysis in the Fuzzy Controller to generate the formulation to find out the relative values of crack depth and crack length from the three inputs of relative values of first, second and third modal frequencies.
4. Finite Element formulation of the same to correlate the data obtained

In the First stage of the research single and double transverse cracks are included for developing the analytical expressions on dynamic characteristics of structures. These cracks introduce new boundary conditions for the structures at the crack locations. These boundary conditions are derived from the strain energy equation using Castigliano's theorem. Presence of crack also reduces stiffness of the structures which has been derived from stiffness matrix. The detailed analyses of crack modelling and stiffness matrices are presented in subsequent sections.

Euler-Bernoulli beam theory is used for dynamic characteristics of beams with transverse cracks. Modified boundary conditions due to presence of cracks, have been used to find out the theoretical expressions for natural frequencies for the beams.

In the second stage a Fuzzy Controller is developed with three input parameters which are relative values of first, second and third mode natural frequencies. And the outputs are relative crack depth and relative crack location. The training data for developing the same is taken from the experimental analysis.

In the third stage Finite Element formulation is performed for the single and double transverse cracks of the cantilever beam. The analysis is performed using certified ALGOR software and the relative values of first, second and third natural frequencies are obtained for comparison.

In the last stage of the investigation the effect of crack depth and crack location on the modal values of natural frequencies are obtained with a very convincing manner. And the data obtained from the Numerical analysis, Fuzzy- Controller analysis and Experimental analysis are compared. Suitable numerical methods are used in order to solve the theoretical equations developed. Useful conclusions are drawn from the numerical results of respective sections. The numerical results are validated by using the experiments on beams and rotors in the corresponding sections. Both the numerical and experimental results are compared and good agreements are obtained.

1.3 Outline of the Thesis

The processes as outlined in this thesis are broadly divided into seven chapters. The current chapter is the first one which deals with the introductory aspect of the thesis. The second chapter contains up-to-date information on literature surveyed on various aspects of vibration analysis of cracked structures, vibration analysis of cracked cantilever beam. The third chapter deals with the theoretical analysis for the Free and Forced Vibration of the both single and double cracked cantilever beam and contains the following sections.

1. Governing Equation for the free vibration analysis.
2. Governing Equation for forced vibration analysis.

The fourth chapter deals with the Fuzzy-Controller analysis to train the data obtain from the experimental analysis to generalize the relation so that relative values of crack depths and crack length can be obtained.

The fifth chapter deals with the Finite Element formulation of the cracked beam to obtain the modal natural frequencies in which the governing equations are obtained for both cracked and uncracked beam.

Chapter 6 represents the detailed discussions on the results obtained from the Fuzzy-Controller, numerical and experimental analysis. The last chapter deals with concluding remarks drawn from the discussions and applications along with the scope for further work.

Chapter 2

Literature Review

2. Literature Review

Cracks are a potential source of catastrophic failure in mechanical machines and in civil structures and in aerospace engineering. To avoid the failure caused by cracks, many researchers have performed extensive investigations over the years to develop structural integrity monitoring techniques. Most of the techniques are based on vibration measurement and analysis because, in most cases, vibration based methods can offer an effective and convenient way to detect fatigue cracks in structures. It is always require that structures must safely work during its service life, however damage initiates a breakdown period on the structures. It is unanimous that cracks are among the most encountered damage types in structures. Crack in structures may be hazardous due their dynamic loadings. So crack detection plays an important for structural health monitoring applications. As Beams type structures are being commonly used in steel construction and machinery industries, focus of the present research work was to develop a newer technique for crack identification and localization. In the Literature Review several studies based on structural health monitoring for crack detection is being discussed. Damage in the form of crack affects the natural frequencies and modes shapes of vibrating beam. The deviations of natural frequencies and modes shapes mainly dependant on location and intensity of the crack.

An analytical study have been performed by Yang et al. [1] on the free and forced vibration of inhomogeneous Euler–Bernoulli beams containing open edge cracks. The beam was subjected to an axial compressive force and a concentrated transverse load moving along the longitudinal direction. Analytical solutions of natural frequencies and dynamic deflections were obtained for cantilever, hinged–hinged, and clamped–clamped beams whose material properties follow an exponential through-thickness variation. It was found that the natural frequencies decrease and the dynamic deflection increases due to the presence of the edge crack and the axial compressive force. While the natural frequencies were greatly influenced by the edge crack, especially when it was located at some specific positions, the dynamic deflection was not very sensitive to the presence and the location of the edge crack. Both free vibration and dynamic response were much more affected by the axial compression than by the edge crack.

Orhan [2] performed a free and forced vibration analysis of a cracked beam in order to identify the crack in a cantilever beam. Single and two-edge cracks were evaluated. The analysis reveals that free vibration analysis provides suitable information for the detection of single and double cracks, whereas forced vibration can detect only single crack condition. However dynamic response of the forced vibration better describes the changes in crack depth and location than the free vibration.

Damage in a cracked structure was analyzed using genetic algorithm technique by Taghi et al. [3]. For modeling the cracked-beam structure an analytical model of a cracked cantilever beam was utilized and natural frequencies were obtained through numerical methods. A genetic algorithm is utilized to monitor the possible changes in the natural frequencies of the structure. The identification of the crack location and depth in the cantilever beam was formulated as an optimization problem.

Theoretical and experimental dynamic behavior of different multi-beams systems containing a transverse crack has been performed by Saavedra and Cuitino [4]. In the crack vicinity the additional flexibility generated by it was being evaluated by strain energy density function which was taken from the linear fracture mechanics theory. A new cracked stiffness matrix is deduced based on flexibility and this can be used subsequently in the FEM analysis of crack systems

Bakhary et al. [5] used Artificial Neural Network for damage detection. In his analysis an ANN model was created by applying Rosenblueth's point estimate method verified by Monte Carlo simulation, the statistics of the stiffness parameters were estimated. The probability of damage existence (PDE) was then calculated based on the probability density function of the existence of undamaged and damaged states. The developed approach was applied to detect simulated damage in a numerical steel portal frame model and also in a laboratory tested concrete slab. The numerical and experimental results demonstrated that, compared with the normal ANN approach, the statistical ANN approach gives more reliable identification of structural damage.

Friswell et al. [6] applied genetic algorithm to the problem of damage detection using vibration data. The objective was to identify the position of one or more damage sites in a structure, and to estimate the extent of the damage at these sites. The genetic

algorithm was used to optimize the discrete damage location variables. For a given damage location site or sites, a standard eigensensitivity method was used to optimize the damage extent. This two-level approach incorporates the advantages of both the genetic algorithm and the eigensensitivity methods. The method was demonstrated on a simulated beam example and an experimental plate example. And Damage at one and two sites have been successfully located in the simulated example of a cantilever beam and also in the experimental cantilever plate. The algorithm was robust to systematic errors in the measured data, demonstrated in simulation by the addition of a discrete mass and experimentally by using a crude model for the plate.

A comprehensive analysis of the stability of a cracked beam subjected to a follower compressive load was presented by Wang [7]. The beam was fixed at its left end and restrained by a translational spring at its right end. The vibration analysis on such cracked beam was conducted to identify the critical compression load for flutter or buckling instability based on the variation of the first two resonant frequencies of the beam. Besides, the effect of the crack's intensity and location on the buckling or flutter compressive load was studied through comprehensive mechanics analysis. And it was observed from the analysis that for flutter instability, flutter load will decrease if the crack is located in the region with positive curvature and increase otherwise to a greater extent compared with that of a healthy beam. On the contrary, for buckling instability, the buckling load will increase if the crack is located in the region with positive curvature and decrease otherwise.

Chondros et al. [8] have developed a continuous cracked beam vibration theory for the lateral vibration of cracked Euler-Bernoulli beams with single-edge or double-edge open cracks. In his approach the Hu-Washizu-Barr variational formulation was used to develop the differential equation and the boundary conditions of the cracked beam as a one-dimensional continuum. The displacement field about the crack was used to modify the stress and the displacement field throughout the bar. The crack was modeled as a continuous flexibility using the displacement field in the vicinity of the crack, found with fracture mechanics methods. The results of the two independent evaluations of the lowest natural frequency of lateral vibrations for beams with a single-edge crack are presented.

And it was observed that the experimental results from aluminum beams with large fatigue cracks are very close to the value predicted.

A new method for natural frequency analysis of beam with an arbitrary number of cracks has been developed by Khiem and Lien [9] on the bases of the transfer matrix method and rotational spring model of crack. The resulted frequency equation of a multiple cracked beam was general with respect to the boundary conditions including the more realistic (elastic) end supports and can be constructed analytically by using symbolic codes. The procedure proposed was advanced by elimination of numerical computation of the high order determinant so that the computational time for calculating natural frequencies in consequence was significantly reduced. Numerical computation has been carried out to investigate the effect of each crack, the number of cracks and boundary conditions on the natural frequencies of a beam. And it was observed that the natural frequencies were sensitive to the elastic boundary conditions only for spring constants ranged in some limited interval. Outside the interval the number of cracks has a more significant effect on the natural frequencies.

Cam et al. [10] have performed a study to obtain information about the location and depth of the cracks in cracked beam. For this purpose the vibrations as a result of impact shocks were analyzed and the signals obtained in defect-free and cracked beams were compared in the frequency domain. The result of the study was suggested to determine the location and depth of cracks by analyzing from the vibration signals. Experimental results and simulations obtained by the software ANSYS were in good agreement.

The relative sensitivities of structural dynamical parameters were analyzed by Hesheng et al. [11] using a directive derivation method. Neural network was used for this purpose. The combined parameters were presented as the input vector of the neural network, which computed with the change rates of the several former natural frequencies (C), the change ratios of the frequencies (R), and the assurance criterions of flexibilities (A). Some numerical simulation examples, such as, cantilever and truss with different damage extends and different damage locations were analyzed. The results indicated that

the combined parameters were more suitable for the input patterns of neural networks than the other parameters alone.

A numerical technique based on the global-local hybrid spectral element (HSE) method was proposed by Hu et al. [12] to study wave propagation in beams containing damages in the form of transverse and lateral cracks. For this purpose spectral element method was employed to model the exterior or far field regions, while a new type of element (HSE) was constructed to model the interior region containing damages. This method was employed to investigate the behaviors of wave propagation in beams containing various types of damages, such as multiple transverse cracks and lateral cracks. With this balanced approach, accurate analyses can be realized with a very coarse FE mesh. And it was observed that the proposed HSEs were highly efficient and can be used to model complex problems.

Wave vibration analysis of an axially loaded cracked Timoshenko beam have been performed by Mei et al. [13]. Axial loading, shear deformation and rotary inertia criteria were considered in this analysis. The transmission and reflection matrices for various discontinuities on an axially loaded Timoshenko beam and the matrix relations between the injected waves and externally applied forces and moments were derived. These matrices were combined to provide a concise and systematic approach to both free and forced vibration analyses of complex axially loaded Timoshenko beams with discontinuities such as cracks and sectional changes.

Analytical predictions of natural frequencies of cracked simply supported beam with a stationary roving mass have been performed by Zhong and Oyadiji [14] in which the natural frequencies of the damaged simply supported beam were studied and the transverse deflection of the cracked beam was constructed by adding a polynomial function, which represents the effects of a crack, to the polynomial function which represents the response of the intact beam. Approximate closed-form analytical expressions were derived for the natural frequencies of an arbitrary mode of transverse vibration of a cracked simply supported beam with a roving mass using the Rayleigh's method. The natural frequencies change due to the roving of the mass along the cracked beam. Therefore the roving mass can provide additional spatial information for damage

detection of the beam. That is, the roving mass can be used to probe the dynamic characteristics of the beam by roving the mass from one end of the beam to the other. The presence of a crack caused the local stiffness of the beam to decrease which, in turn, caused a marked decrease in natural frequency of the beam when the roving mass was located in the vicinity of the crack. The magnitude of the roving mass used was varied between 0% and 50% of the mass of the beam. The predicted frequencies were compared very well with those obtained using the finite element method and the experimental results.

Artificial Intelligence tools such as neural network, genetic algorithm and fuzzy logic have been used by Saridakis et al. [15] for identification of cracks in shafts using coupled response measurements. In this research the dynamic behavior of a shaft with two transverse cracks characterized by three measures: position, depth and relative angle. Both cracks were considered to lie along arbitrary angular positions with respect to the longitudinal axis of the shaft and at some distance from the clamped end. A local compliance matrix of two degrees of freedom (bending in both the horizontal and the vertical planes) was used to model each crack. The calculation of the compliance matrix was based on established stress intensity factor expressions and was performed for all rotation angles through a function that incorporated the crack depth and position as parameters. Towards this goal, five different objective functions were proposed and validated; two of these were based on fuzzy logic. More computational intelligence was added through a genetic algorithm, which was used to find the characteristics of the cracks through artificial neural networks that approximate the analytical model. Both the genetic algorithm and the neural networks contributed to a remarkable reduction of the computational time without any significant loss of accuracy. The final results showed that the proposed methodology may constitute an efficient tool for real-time crack identification.

Another novel approach for crack detection in beam like structures using RBF (Radial Basis Function) neural network have been performed by Huijian et al. [16] with an experimental validation. In the particular research a crack damage detection algorithm was presented using a combination of global and local vibration-based analysis data as input in artificial neural networks (ANNs) for location and severity prediction of crack

damage in beam like structures. Finite element analysis has been used to obtain the dynamic characteristics of intact and damaged cantilever steel beams for the first three natural modes. In the experimental analysis, several steel beams with six distributed surface bonded electrical strain gauges and an accelerometer mounted at the tip have been used to obtain modal parameters such as resonant frequencies and strain mode shapes. Finally, the Radial Basis Function ANNs have been trained using the data obtained from the numerical damage case to predicate the severity and localization of the crack damage.

A new concept of nonlinear output frequency response functions (NOFRFs) has been introduced by Peng et al. [17] to detect cracks in beams using frequency domain information and the results showed that the NOFRFs were a sensitive indicator of the presence of cracks providing the excitation is of an appropriate intensity. They also constitute an indicative and promising basis, which must further be explored, so that the method can be used for the detection of cracks in beams with applications in structural fault diagnosis.

Damage identification based on propagating Lamb wave measurements have been introduced by Grabowska et al. [18] which has been developed especially for distinguishing different kinds of damages. The reason for the research was that for example small voids in material, classified as damage, do not influence its overall strength. The usage of wavelet transformation with propagating Lamb waves for distinguishing between different failures was the most important novelty of the research done. To obtain the presented results for modeling, the FFT-based spectral element method has been used. And for signal processing, the wavelet analysis has been employed.

Crack identification in beam by dynamic response has been proposed by Law and Lu [19] by using time domain. The crack was modeled as a discrete open crack represented mathematically by the Dirac delta function. The dynamic responses were calculated basing on modal superposition. In the inverse analysis, optimization technique coupled with regularization on the solution was used to identify the crack(s). The formulation for identification was further extended to the case of multiple cracks. A

general orthogonal polynomial function was used to generate the derivatives of the strain or displacement time responses to eliminate the error due to measurement noise. Computation simulations with sinusoidal and impulsive excitations on a beam with a single crack or multiple cracks showed that the method was effective for identifying the crack parameters with accuracy. The proposed identification algorithm was also verified experimentally from impact hammer tests on a beam with a single crack.

Pawar et al. [20] have proposed spatial Fourier analysis and Neural technique for damage detection in beam. The study investigated the effect of damage on beams with fixed boundary conditions using Fourier analysis of mode shapes in the spatial domain. A finite element model was used to obtain the mode shapes of a damaged fixed–fixed beam, and the damaged mode shapes were expanded using a spatial Fourier series and the effect of damage on the harmonics was investigated. This approach was contrasted with the typical time domain application of Fourier analysis for vibration problems. It was found that damage caused considerable change in the Fourier coefficients of the mode shapes, which were found to be sensitive to both damage size and location. Therefore, a damage index in the form of a vector of Fourier coefficients was formulated. A neural network was trained to detect the damage location and size using Fourier coefficients as input. Numerical studies showed that damage detection using Fourier coefficients and neural networks has the capability to detect the location and damage size accurately.

Free and Forced response measurement method has been proposed by Karthikeyan et al. [21] which gave crack flexibility coefficients as a by-product. Timoshenko beam theory was used in the beam modeling for transverse vibrations. The finite element method (FEM) was used for the cracked beam free and forced vibration analysis. An open transverse surface crack was considered for the crack model. The effect of the proportionate damping has been included. A harmonic imbalance force of known amplitude and frequency was used to dynamically excite the beam with the help of an independent exciting unit. The crack localisation and sizing algorithm was iterative in nature. The iteration started with an initial guess for the crack depth ratio and iteratively estimated the crack location and the crack depth until the desired convergence for both the crack location and the crack depth were obtained. For estimation of bounded flexibility coefficients, a regularization technique has been adopted. The prediction of the

crack location and size were in good agreement even in the presence of the measurement error and noise.

Ostachowicz [22] have proposed Spectral finite element method for crack detection in structures. The research brought together the principles, equations, and applications of damage modeling and elastic waves propagation, both traditional and state-of-the-art in a review form. It began with the relevant fundamentals of damage modeling, by deriving the basic equations of fracture mechanics and elastic wave propagations, and applications of Lamb waves was covered that has been at the forefront of today's research. The results obtained indicated that the current approach was capable of detecting cracks and delaminations of very small size, even in the presence of considerable measurement errors.

Parhi and Das [23] introduced newest technique known as Fuzzy-Gaussian interference Technique for crack detection in cracked cantilever beam. The fuzzy-logic controller used in the present investigation consisted of six input parameters and two output parameters. The input parameters to the fuzzy controller were the relative divergence of the first three natural frequencies and first three mode shapes in dimensionless forms. The output parameters of the fuzzy controller were the relative crack depth and relative crack location in dimensionless forms. Theoretical expressions have been developed to derive the fuzzy rules for the controller considering four parameters such as natural frequencies, mode shapes, crack depths, and crack locations. The strain-energy release rate method has been used for calculating the local stiffnesses of the beam for a mode-I type of the crack. Several boundary conditions were outlined that take into account the crack location. Required fuzzy rules were derived for the fuzzy Gaussian controller. The experimental setup has been fabricated in the laboratory for verifying the robustness of the developed fuzzy controller. The developed fuzzy controller has been able to predict the location and depth of the crack in close proximity with the real results.

An analytical, as well as experimental approach to the crack detection in cantilever beams

using vibration analysis has been established by Nahvi and Jabbari [24]. In the approach an experimental setup was designed in which a cracked cantilever beam was excited by a hammer and the response was obtained using an accelerometer attached to the beam. To avoid non-linearity, it was assumed that the crack was always open. To identify the crack, contours of the normalized frequency in terms of the normalized crack depth and location were plotted. The intersection of contours with the constant modal natural frequency planes was used to relate the crack location and depth. A minimization approach was employed for identifying the cracked element within the cantilever beam. The proposed method was based on measured frequencies and mode shapes of the beam.

A method for crack identification in double-cracked beams based on wavelet analysis has been presented by Loutridis et al. [25] in which the fundamental vibration mode of a double-cracked cantilever beam was analyzed using continuous wavelet transform and both the location and depth of the cracks were estimated. The location of the cracks was determined by the sudden changes in the spatial variation of the transformed response. To estimate the relative depth of the cracks, an intensity factor was established which correlated the size of the cracks to the coefficients of the wavelet transform. It was shown that the intensity factor followed definite trends and therefore can be used as an indicator for crack size. The proposed technique was validated both analytically and experimentally in case of a double-cracked cantilever beam having cracks of varying depth at different positions. In the light of the obtained results, the advantages and limitations of the method were presented and discussed.

The aero-elastic characteristics of a cantilevered composite panel of large aspect ratio and with an edge crack are investigated by Wang et al. [26]. The panel consists of several fiber-reinforced composite plies, and was modeled with a one-dimensional beam vibrating in coupled bending and torsion. The fundamental mode shapes of the cracked cantilever were used to study the interaction between a crack and aerodynamic characteristics by employing Galerkin's method. Variation of the divergence/flutter speed with respect to the crack ratio, its location as well as the fiber angle was also investigated. The divergence/ flutter speed was more sensitive to the bending–torsion coupling parameter than to the presence of the crack. The crack may or may not reduce the divergence/flutter speed, depending on the fiber orientation. And it was observed that the

qualitative analysis may help the development of an online prognosis tool for an aircraft with large aspect-ratio unswept composite wings.

Damage assessment in structures from changes in static parameter using neural network have been performed by Maity and Saha [27] in their study. The basic strategy applied in this study was to train a neural network to recognize the behaviour of the undamaged structure as well as of the structure with various possible damaged states. When this trained network was subjected to the measured response, it was able to detect any existing damage. The idea was applied on a simple cantilever beam. Strain and displacement were used as possible candidates for damage identification by a back-propagation neural network and the superiority of strain over displacement for identification of damage has been observed.

Identifying the locations and severity of damage in structures using frequency response function (FRF) data have been formulated by Hwang and Kim [28]. The basic method followed to detect the location and severity by minimizing the difference between test and analytic FRFs, which was a type of model updating or optimization method; however, the preferred method proposed in this study used only a subset of vectors from the full set of FRFs for a few frequencies and the stiffness matrix and reductions in explicit form was calculated. To verify the proposed method, examples for a simple cantilever and a helicopter rotor blade were numerically demonstrated. The proposed method identified the location of damage in these objects, and characterized the damage to a satisfactory level of precision.

An analysis has been performed by Patil and Maiti [29] for the detection of multiple cracks using frequency measurements. The method is based on transverse vibration modelling through transfer matrix method and representation of a crack by rotational spring. The beam was virtually divided into a number of segments, which can be decided by the analyst, and each of them was considered to be associated with a damage parameter. The procedure gave a linear relationship explicitly between the changes in natural frequencies of the beam and the damage parameters. These parameters were determined from the knowledge of changes in the natural frequencies. After obtaining them, each was treated in turn to exactly pinpoint the crack location in the

segment and also determined its size. The forward, or natural frequency determination, problems were examined in the passing. Though approximate but the method has been capable to handle segmented beams, any boundary conditions, intermediate spring or rigid supports, etc. It also eliminated the need for any symbolic computation.

Analysis for detection of the location and size of the cracks has been performed by Chang and Chen [30]. The proposed analysis was able to calculate both the positions and depths of multi-cracks from spatial wavelet based method. First, the mode shapes of free vibration and natural frequencies of the multiple cracked beams were obtained. The crack type was open crack and was represented as a rotational spring. Then the mode shapes were analyzed by wavelet transformation to get the positions of the cracks. When the positions of the cracks have been known from the plot of wavelet coefficients, the natural frequencies can be used to predict the depth of the cracks through the characteristic equation. If the number of cracks is n ; the first n natural frequencies were used to predict the depth of the cracks. It was observed that the positions and depths of the cracks can be predicted with acceptable precision even though there are many cracks in the beam.

Cracked beam element method for structural analysis has been used by Viola et al. [31] for detection of crack location. The remarks involved from the analysis was that the local flexibility introduced by cracks changes the dynamic behavior of the structure and by examining this change, crack position and magnitude can be identified. In order to model the structure for FEM analysis, a special finite element for a cracked Timoshenko beam was developed. Shape functions for rotational and translational displacement were used to obtain the consistent mass matrix for the cracked beam element. Effect of the cracks on the stiffness matrix and consistent mass matrix was investigated and the cracks in the structure were identified using the modal data.

Dynamic stiffness matrix to calculate the natural frequencies and normal mode shapes of uniform isotropic beam element have been developed by Li et al. [32] based on trigonometric shear deformation theory. The theoretical expressions for the dynamic stiffness matrix elements were found directly, in an exact sense, by solving the governing differential equations of motion that described the deformations of the beam element

according to the trigonometric shear deformation theory, which included the sinusoidal variation of the axial displacement over the cross section of the beam. The numerical results obtained are compared to the available solutions wherever possible and validate the accuracy and efficiency of the present approach.

Han et al. [33] have proposed a method for analyzing the dynamics of transversely vibrating beam using four theories which were: Euler-Bernoulli, Rayleigh, shear and Timoshenko. In the investigation four models for the transversely vibrating beam were prepared and the equation of motion for each model, and the expressions for boundary conditions were obtained using Hamilton's variational principle. The frequency equations were obtained for four sets of end conditions: free-free, clamped-clamped, hinged-hinged and clamped-free. The roots of the frequency equations were presented in terms of normalized wave numbers. The normalized wave numbers for the other six sets of end conditions were obtained using the analysis of symmetric and anti-symmetric modes. Then the orthogonality conditions of the eigen-functions or mode shape and the procedure to obtain the forced response using the method of eigen-function expansion was presented.

A robust iterative algorithm has been used by Xu et al. [34] for identifying the locations and extent of damage in beams using only the changes in their first several natural frequencies. The algorithm, which was a combination of a first-order, multiple-parameter perturbation method and the generalized inverse method, was tested extensively through experimental and numerical means on cantilever beams with different damage scenarios. If the damage was located at a position within 0–35% or 50–95% of the length of the beam from the cantilevered end, while the resulting system equations were severely underdetermined, the minimum norm solution from the generalized inverse method lead to a solution that closely represented the desired solution at the end of iterations when the stiffness parameters of the undamaged structure were used as the initial stiffness parameters. If the damage was located at a position within 35–50% of the length of the beam from the cantilevered end, the resulting solution by using the stiffness parameters of the undamaged structure as the initial stiffness parameters deviates significantly from the desired solution. In this case, a new method was developed to enrich the measurement information by modifying the structure in a

controlled manner and using the first several measured natural frequencies of the modified structure. A new method using singular value decomposition was also developed to handle the ill-conditioned system equations that occurred in the experimental investigation by using the measured natural frequencies of the modified structure.

Waveform fractal dimension has been proposed by Qiao and Cao [35] for mode shape-based damage identification of beam-type structures. In the analysis a mathematical solution on the use of applying waveform fractal dimension to higher mode shapes for crack identification has been proposed, from which the inherent deficiency of waveform fractal dimension to identify crack when implemented to higher mode shapes was overcome. The applicability and effectiveness of the AWCD-MAA was validated by an experimental program on damage identification of a cracked composite cantilever beam using smart piezoelectric sensors/actuators (i.e., piezoelectric lead–zirconate–titanate (PZT) and polyvinylidene fluoride (PVDF)). The proposed AWCD-MAA provided a novel, viable method for crack identification of beam-type structures without baseline requirement, and it expanded the scope of fractal in structural health monitoring applications.

A new method of vibration-based damage identification in structures exhibiting axial and torsional responses has been proposed by Duffey et al. [36]. The method has been derived to detect and localize linear damage in a structure using the measured modal vibration parameters and was applicable when the vibration strain energy has been stored in the axial or torsional modes, which differentiated it from previously derived strain-energy-based methods. The new method was then compared to the previously derived flexibility-change method. Both methods were verified by application to an analytical eight degree of freedom model. Experimental validation for both methods was also presented by application to an experimental eight degree of freedom spring-mass structure.

Different crack identification techniques have been discussed briefly by Dimarogonas [37]. And it has been summarized in that attempt that the presence of a crack in a structural member introduced a local flexibility that used to affect its vibration

response. Moreover, the crack will open and close in time depending on the rotation and vibration amplitude. In this case the system was nonlinear. Furthermore, if general motion has been considered, the local stiffness matrix description of the cracked section of the shaft lead to a coupled system, while for an uncracked shaft the system was decoupled. This means that the crack introduced new harmonics in the spectrum. In fact, in addition to the second harmonic of rotation and the subharmonic of the critical speed, two more families of harmonics are observed: (1) higher harmonics of the rotating speed due to the nonlinearity of the closing crack, and (2) longitudinal and torsional harmonics are present in the start-up lateral vibration spectrum due to the coupling.

For beams containing multiple cracks and subjected to axial force a new method has been proposed by Binici [38] which used a set of end conditions as initial parameters for determining the mode shape functions. Satisfying the continuity and jump conditions at crack locations, mode shape functions of the remaining parts were determined. Other set of boundary conditions yielded a second-order determinant that need to be solved for its roots. As the static case was approached, the roots of the characteristic equation gave the buckling load of the structure. The proposed method was compared against the results predicted by finite element analysis and a good agreement was observed between the proposed approach and finite element results. A parametric study was conducted in order to investigate the effect of cracks and axial force levels on the eigenfrequencies. Both simply supported and cantilever beam-columns were considered for this purpose. It is has been found that eigenfrequencies were strongly affected by crack locations, severities and axial force levels. Simple modifications to account for flexible intermediate supports were presented as well. The proposed method can efficiently be used in detecting crack locations, severities and axial forces in beams and columns. Furthermore it can be used to predict the critical load of damaged structures based on eigenfrequency measurements.

A continuous cracked bar vibration model of a cracked Euler-Bernoulli cantilevered beam with an edge crack has been formulated by Chondros and Dimarogonas [39] in which the Hu-Washizu-Barr variational formulation was used to develop the differential equation and the boundary conditions for the cracked beam as an one-dimensional continuum. The crack has been modelled as a continuous flexibility using the displacement field in the vicinity of the crack found with fracture mechanics

methods. And the results of the three independent evaluations of the lowest natural frequency of the aluminum cantilever beam with a single-edge crack were presented. The experimental result was found to be being very close to the values predicted by the continuous cracked beam formulation. And it has been observed that the continuous cracked beam theory agrees with the experimental results than the lumped crack flexibility theory.

Vibration based structural damage detection in flexural members using multi-criteria approach has been presented by Shih et al. [40]. In the analysis computer simulation techniques have been developed and applied a procedure using non-destructive methods for damage assessment in beams and plates, which are important flexural members in building and bridge structures. In addition to changes in natural frequencies, two methods, called the modal flexibility and the modal strain energy method have been incorporated which were based on the vibration characteristics of the structure. Using the results from modal analysis, algorithms based on flexibility and strain energy changes before and after damage were obtained and used as the indices for the assessment of the status of the structural health. The objective of the analysis was to evaluate the feasibility of the proposed multi-criteria method to identify and localize single and multiple damages in numerical models of flexural members having different boundary conditions. The application of the approach was demonstrated through two sets of numerical simulation studies on beam and plate structures with nine damage scenarios in each. Results showed that the proposed multi-criteria method incorporating modal flexibility and modal strain energy method was effective in multiple damage assessment in beam and plate structures.

A vibration analysis of multiple-cracked non-uniform beams has been performed by Mazanoglu et al. [41] using the energy-based method. The method has been employed for the vibration analysis of non-uniform Euler-Bernoulli beams having multiple open cracks which included the distribution of the energy consumed determined by taking into account not only the strain change at the cracked beam surface as in general but also the considerable effect of the stress field caused by the angular displacement of the beam due to bending. The Rayleigh–Ritz approximation method has been used in the analysis. The method was adapted to the cases of multiple cracks with an approach based on the

definition of strain disturbance variation along the beam. Examples were presented on cantilever beams having different truncation factors. And the results were then compared with a commercial finite element programme and with that of the method used via modified Fourier series resulting encouraging agreements.

A robust fault detection method has been formulated by McAdams and Tumer [42] for the damage assessment of turbine blades. Specifically in the approach the combined impact of crack damage and manufacturing variation on the vibrational characteristics of turbine blades modeled as pinned-pinned beams has been explored. The changes in the transverse vibration and associated eigenfrequencies of the beams were considered. A complete variational beam vibration model was developed and presented that allows variations in geometry and material properties to be considered, with and without crack damage. To simplify variational simulation, separation of variables was used for fast simulations. This formulation has been presented in detail. To establish a baseline of the effect of geometric variations on the system vibrational response, a complete numerical example was presented that included damaged beams of ideal geometry and damaged beams with geometric variation. It has been observed that changes in fault detection monitoring signals caused by geometric variation were small with those caused by damage and impending failure. Also, when combined, the impact of geometric variation and damage appear to be independent.

Structural damage detection using transfer matrix method has been performed by Escobar et al. [43] in which a method for locating and estimating structural damage in two and three-dimensional analytical models of buildings was presented. Since the geometrical transformation matrix used to obtain the condensed stiffness matrix of a structure can be estimated, for the damaged state, from the one corresponding to the non-damaged state with an iterative scheme, it was possible to detect structural damage by comparing changes on structural dynamic parameters, modal shapes and vibration frequencies with their defining properties. The application and accuracy of the method was then illustrated by means of numerical analyses of building models.

A new damage detection technique has been formulated by Fang et al. [44] using neural network with learning rate improvement. In the research structural damage

detection using frequency response functions (FRFs) as input data to the back-propagation neural network (BPNN) has been explored. Such method was non-model based and thus could have advantage in many practical applications. Neural network based damage detection generally consisted of a training phase and a recognition phase. Error back-propagation algorithm incorporating gradient method has been applied to train the neural network, whereas the training efficiency heavily depended on the learning rate. While various training algorithms, such as the dynamic steepest descent (DSD) algorithm and the fuzzy steepest descent (FSD) algorithm, have shown promising features (such as improving the learning convergence speed), their performance is hinged upon the proper selection of certain control parameters and control strategy. In the particular attempt tunable steepest descent (TSD) algorithm using heuristics approach, which improves the convergence speed significantly without sacrificing the algorithm simplicity and the computational effort, was investigated. A series of numerical examples demonstrate that the proposed algorithm outperforms both the DSD and FSD algorithms. With this as basis, the neural network has been implemented to the FRF based structural damage detection. The analysis resulted on a cantilevered beam show that, in all considered damage cases (i.e., trained damage cases and unseen damage cases, single damage cases and multiple-damage cases), the neural network was able to assess damage conditions with very good accuracy.

Different studies on double/multi-cracks has been summarized by Sekhar [45] and the respective influences, identification methods in vibration structures as beams, rotors, pipes etc. were discussed. This particular study brought out the state of the research on multiple cracks and their identification.

A novel nondestructive damage detection method has been developed by Hearndon et al. [46] to study the influence of a crack on the dynamic properties of a cantilever beam subjected to bending. Experimental measurements of transfer functions for the cracked cantilever beam revealed a change in the natural frequency with increasing crack length. A finite element model of a cracked element was created to compute the influence of severity and location of damage on the structural stiffness. The proposed model was based on the response of the cracked beam element under a static load. The change in beam deflection as a result of the crack was used to calculate the

reduction in the global component stiffness. The reduction of the beam stiffness was then used to determine its dynamic response employing a modal analysis computational model. Euler–Bernoulli and Timoshenko beam theories were used to quantify the elastic stiffness matrix of a finite element. The transfer functions from both theories compared well with the experimental results. The experimental and computational natural frequencies decreased with increasing crack length. Furthermore the Euler–Bernoulli and Timoshenko beam theories resulted in approximately the same decrease in the natural frequency with increasing crack length as experimentally measured.

Identification of multiple cracks in a beam has been presented by Lee [47] in which the cracks were modeled as rotational springs and the forward problem was solved using the finite element method. The inverse problem was solved iteratively for the locations and sizes of the cracks using the Newton–Raphson method. Numerical examples have been provided for the identification of triple cracks in a cantilever beam as well as double cracks. The detected crack locations and sizes were in excellent agreement with the actual ones.

Flexural wave propagation characteristics have been used by Park [48] for identification of damage in beam structures. In the analysis an experimental method of detecting damage using the flexural wave propagation characteristics was proposed. To monitor change in structural properties due to damage, the frequency-dependent variation of the wavenumber, wave speed, and the dynamic properties were measured in the frequency ranges of flexural vibration. The measured frequency dependent variation was compared to those measured when undamaged. The beam transfer function method was used to obtain the dynamic properties. The location and magnitude of damage were identified using the property that it had significant impact on the system potential energy. When the wave propagates through a medium, the total system energy remained mostly unchanged, but its form changes between potential and kinetic energy. The wave propagation characteristics were affected most when damage occurs at locations where the wave energy was in the form of the potential energy. The validity of the proposed method was confirmed by experimentation. The various locations of damage imposed on the beam structures with different magnitudes were identified accurately.

Chapter 3

Theoretical Analyses

3. Theoretical Analyses

3.1 Local flexibility of a Cracked Beam under Bending and Axial Loading

The presence of a transverse surface crack of depth 'a1' on beam of width 'B' and height 'W' introduces a local flexibility, which can be defined in matrix form, the dimension of which depends on the degrees of freedom. Here a 2x2 matrix is considered. A cantilever beam is subjected to axial force (P1) and bending moment (P2), shown in figure 1a, which gives coupling with the longitudinal and transverse motion.

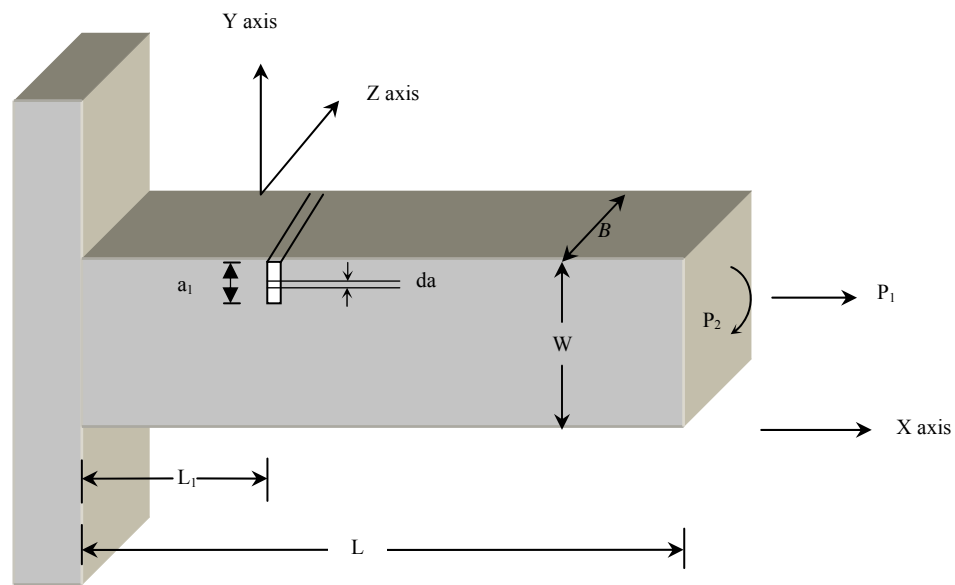


Fig. 3.1 (a) Geometry of The Cracked Cantilever Beam

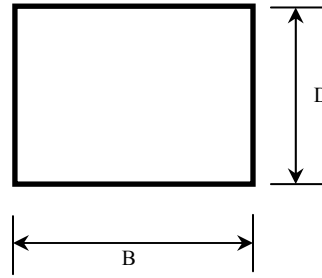


Fig. 3.1 (b) Cross-sectional View of the Beam

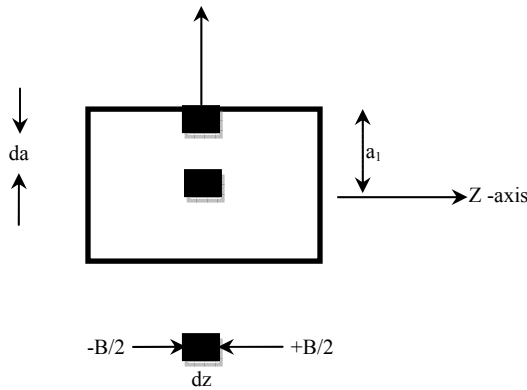


Fig. 3.1 (c) Segments taken during Integration at the Crack section

The strain energy release rate at the fractured section can be written as (Tada et al., 1973);

$$J = \frac{1}{E'} (K_{I1} + K_{I2})^2, \text{ Where } \frac{1}{E'} = \frac{1-\nu^2}{E'} \text{ (for plane strain condition);}$$

$$= \frac{1}{E} \text{ (for plane stress condition)}$$

K_{I1}, K_{I2} are the stress intensity factors of mode I (opening of the crack) for load P_1 and P_2 respectively. The values of stress intensity factors from earlier studies as per Tada et al. [49] are;

$$K_{11} = \frac{P_1}{BW} \sqrt{\pi a} (F_1(\frac{a}{W})), K_{12} = \frac{6P_2}{BW^2} \sqrt{\pi a} (F_2(\frac{a}{W}))$$

Where expressions for F_1 and F_2 are as follows

$$F_1(\frac{a}{W}) = (\frac{2W}{\pi a} \tan(\frac{\pi a}{2W}))^{0.5} \left\{ \frac{0.752 + 2.02(a/W) + 0.37(1 - \sin(\pi a / 2W))^3}{\cos(\pi a / 2W)} \right\}$$

$$F_2(\frac{a}{W}) = (\frac{2W}{\pi a} \tan(\frac{\pi a}{2W}))^{0.5} \left\{ \frac{0.923 + 0.199(1 - \sin(\pi a / 2W))^4}{\cos(\pi a / 2W)} \right\}$$

Let U_t be the strain energy due to the crack. Then from Castigliano's theorem, the additional displacement along the force P_i is:

$$u_i = \frac{\partial U_t}{\partial P_i} \quad (3.1)$$

$$\text{The strain energy will have the form, } U_t = \int_0^{a_1} \frac{\partial U_t}{\partial a} da = \int_0^{a_1} J da \quad (3.2)$$

Where $J = \frac{\partial U_t}{\partial a}$ the strain energy density function.

From (1) and (2), thus we have

$$u_i = \frac{\partial}{\partial P_i} \left[\int_0^{a_1} J(a) da \right] \quad (3.3)$$

The flexibility influence co-efficient C_{ij} will be, by definition

$$C_{ij} = \frac{\partial u_i}{\partial P_j} = \frac{\partial^2}{\partial P_i \partial P_j} \int_0^{a_1} J(a) da \quad (3.4)$$

To find out the final flexibility matrix we have to integrate over the breadth 'B'

$$C_{ij} = \frac{\partial u_i}{\partial P_j} = \frac{\partial^2}{\partial P_i \partial P_j} \int_{-B/2}^{+B/2} \int_0^{a_1} J(a) da dz \quad (3.5)$$

Putting the value strain energy release rate from above, equation (5) modifies as

$$C_{ij} = \frac{B}{E'} \frac{\partial^2}{\partial P_i \partial P_j} \int_0^{a_1} (K_{11} + K_{12})^2 da \quad (3.6)$$

$$\text{Putting } \xi = (a/w), d\xi = \frac{da}{W},$$

We get $da = Wd\xi$ and when $a = 0$, $\xi = 0$; $a = a_1$, $\xi = a_1/W = \xi_1$

From above condition equation (6) converts to,

$$C_{ij} = \frac{BW}{E'} \frac{\partial^2}{\partial P_i \partial P_j} \int_0^{\xi_1} (K_{11} + K_{12})^2 d\xi \quad (3.7)$$

From the equation (7), calculating C_{11} , C_{12} ($=C_{21}$) and C_{22} we get

$$\begin{aligned} C_{11} &= \frac{BW}{E'} \int_0^{\xi_1} \frac{\pi a}{B^2 W^2} 2(F_1(\xi))^2 d\xi \\ &= \frac{2\pi}{BE'} \int_0^{\xi_1} \xi (F_1(\xi))^2 d\xi \end{aligned} \quad (3.8)$$

$$C_{12} = C_{21} = \frac{12\pi}{E'BW} \int_0^{\xi_1} \xi F_1(\xi) F_2(\xi) d\xi \quad (3.9)$$

$$C_{22} = \frac{72\pi}{E'BW^2} \int_0^{\xi_1} \xi F_2(\xi) F_2(\xi) d\xi \quad (3.10)$$

Converting the influence co-efficient into dimensionless form

$$\overline{C}_{11} = C_{11} \frac{BE'}{2\pi} \quad \overline{C}_{12} = C_{12} \frac{E'BW}{12\pi} = \overline{C}_{21} ; \quad \overline{C}_{22} = C_{22} \frac{E'BW^2}{72\pi}$$

The local stiffness matrix can be obtained by taking the inversion of compliance matrix.

i.e.

$$K = \begin{bmatrix} K_{11} & K_{12} \\ K_{21} & K_{22} \end{bmatrix} = \begin{bmatrix} C_{11} & C_{12} \\ C_{21} & C_{22} \end{bmatrix}^{-1}$$

3.2 Analysis of Vibration Characteristics of the Cracked Beam:

3.2.1 Free Vibration

A cantilever beam of length 'L' width 'B' and depth 'W', with a crack of depth 'a1' at a distance 'L1' from the fixed end is considered shown in figure 1. Taking $u_1(x, t)$ and $u_2(x, t)$ as the amplitudes of longitudinal vibration for the sections before and after the crack and $y_1(x, t)$, $y_2(x, t)$ are the amplitudes of bending vibration for the same sections shown in figure 2.

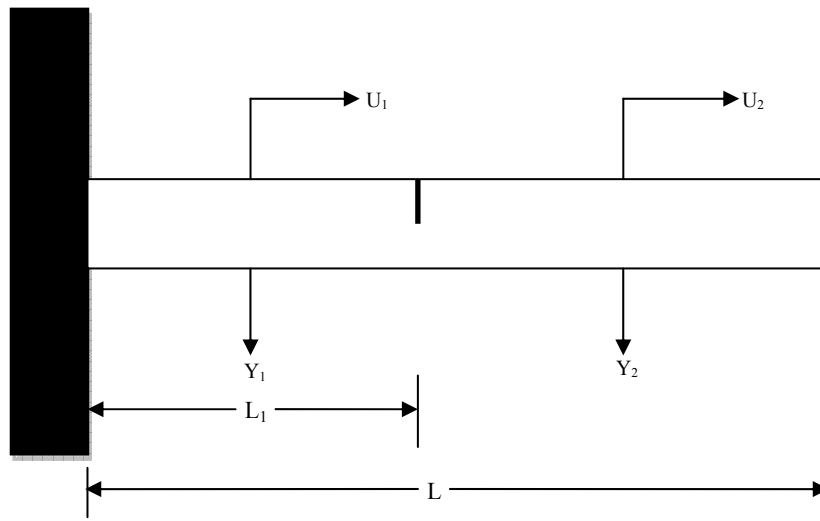


Fig. 3.2 Beam model

A cantilever beam of length 'L' width 'B' and depth 'W', with a crack of depth 'a1' at a distance 'L1' from the fixed end is considered shown in Figure 1. Taking $u_1(x, t)$ and $u_2(x, t)$ as the amplitudes of longitudinal vibration for the sections before and after the

crack and $y_1(x, t)$, $y_2(x, t)$ are the amplitudes of bending vibration for the same sections shown in Figure 3.

The normal function for the system can be defined as

$$\bar{u}_1(\bar{x}) = A_1 \text{Cos}(\bar{K}_u \bar{x}) + A_2 \text{Sin}(\bar{K}_u \bar{x}) \quad (3.11a)$$

$$\bar{u}_2(\bar{x}) = A_3 \text{Cos}(\bar{K}_u \bar{x}) + A_4 \text{Sin}(\bar{K}_u \bar{x}) \quad (3.11b)$$

$$\bar{y}_1(\bar{x}) = A_5 \text{Cosh}(\bar{K}_y \bar{x}) + A_6 \text{Sinh}(\bar{K}_y \bar{x}) + A_7 \text{Cos}(\bar{K}_y \bar{x}) + A_8 \text{Sin}(\bar{K}_y \bar{x}) \quad (3.11c)$$

$$\bar{y}_2(\bar{x}) = A_9 \text{Cosh}(\bar{K}_y \bar{x}) + A_{10} \text{Sinh}(\bar{K}_y \bar{x}) + A_{11} \text{Cos}(\bar{K}_y \bar{x}) + A_{12} \text{Sin}(\bar{K}_y \bar{x}) \quad (3.11d)$$

For double crack case the above formulation will be same except variation in the above equations;

$$\bar{u}_1(\bar{x}) = A_1 \text{Cos}(\bar{K}_u \bar{x}) + A_2 \text{Sin}(\bar{K}_u \bar{x}) \quad (3.12a)$$

$$\bar{u}_2(\bar{x}) = A_3 \text{Cos}(\bar{K}_u \bar{x}) + A_4 \text{Sin}(\bar{K}_u \bar{x}) \quad (3.12b)$$

$$\bar{u}_3(\bar{x}) = A_5 \text{Cos}(\bar{K}_u \bar{x}) + A_6 \text{Sin}(\bar{K}_u \bar{x}) \quad (3.12c)$$

$$\bar{y}_1(\bar{x}) = A_7 \text{Cosh}(\bar{K}_y \bar{x}) + A_8 \text{Sinh}(\bar{K}_y \bar{x}) + A_9 \text{Cos}(\bar{K}_y \bar{x}) + A_{10} \text{Sin}(\bar{K}_y \bar{x}) \quad (3.12d)$$

$$\bar{y}_2(\bar{x}) = A_{11} \text{Cosh}(\bar{K}_y \bar{x}) + A_{12} \text{Sinh}(\bar{K}_y \bar{x}) + A_{13} \text{Cos}(\bar{K}_y \bar{x}) + A_{14} \text{Sin}(\bar{K}_y \bar{x}) \quad (3.11e)$$

$$\bar{y}_3(\bar{x}) = A_{15} \text{Cosh}(\bar{K}_y \bar{x}) + A_{16} \text{Sinh}(\bar{K}_y \bar{x}) + A_{17} \text{Cos}(\bar{K}_y \bar{x}) + A_{18} \text{Sin}(\bar{K}_y \bar{x}) \quad (3.12f)$$

Where $\bar{x} = \frac{x}{L}$, $\bar{u} = \frac{u}{L}$, $\bar{y} = \frac{y}{L}$, $\beta = \frac{L_1}{L}$

$$\bar{K}_u = \frac{\omega L}{C_u}, C_u = \left(\frac{E}{\rho}\right)^{1/2}, \bar{K}_y = \left(\frac{\omega L^2}{C_y}\right)^{1/2}, C_y = \left(\frac{EI}{\mu}\right)^{1/2}, \mu = A\rho$$

A_i , ($i=1, 12$) Constants are to be determined, from boundary conditions. The boundary conditions of the cantilever beam in consideration are:

$$\bar{u}_1(0)=0; \quad \bar{y}_1(0)=0; \quad \bar{y}'_1(0)=0; \quad \bar{u}_2(1)=0; \quad \bar{y}''_2(1)=0; \quad \bar{y}'''_2(1)=0$$

At the cracked section:

$$\bar{u}_1(\beta) = \bar{u}_2(\beta); \quad \bar{y}_1(\beta) = \bar{y}_2(\beta); \quad \bar{y}_1''(\beta) = \bar{y}_2''(\beta); \quad \bar{y}_1'''(\beta) = \bar{y}_2'''(\beta)$$

Also at the cracked section, we have:

$$AE \frac{du_1(L_1)}{dx} = K_{11} (u_2(L_1) - u_1(L_1)) + K_{12} \left(\frac{dy_2(L_1)}{dx} - \frac{dy_1(L_1)}{dx} \right)$$

Multiplying both sides of the above equation by $\frac{AE}{LK_{11}K_{12}}$ we get;

$$M_1 M_2 \bar{u}'(\beta) = M_2 (\bar{u}_2(\beta) - \bar{u}_1(\beta)) + M_1 (\bar{y}_2'(\beta) - \bar{y}_1'(\beta))$$

$$\text{Similarly, } EI \frac{d^2 y_1(L_1)}{dx^2} = K_{21} (u_2(L_1) - u_1(L_1)) + K_{22} \left(\frac{dy_2(L_1)}{dx} - \frac{dy_1(L_1)}{dx} \right)$$

Multiplying both sides of the above equation by $\frac{EI}{L^2 K_{22} K_{21}}$ we get,

$$M_3 M_4 \bar{y}_1''(\beta) = M_3 (\bar{u}_2(\beta) - \bar{u}_1(\beta)) + M_4 (\bar{y}_2'(\beta) - \bar{y}_1'(\beta))$$

$$\text{Where, } M_1 = \frac{AE}{LK_{11}}, \quad M_2 = \frac{AE}{K_{12}}, \quad M_3 = \frac{EI}{LK_{22}}, \quad M_4 = \frac{EI}{L^2 K_{21}}$$

The normal functions, equation (11) along with the boundary conditions as mentioned above, yield the characteristic equation of the system as:

$$|Q| = 0 \tag{3.13}$$

This determinant is a function of natural circular frequency (ω), the relative location of the crack (β) and the local stiffness matrix (K) which in turn is a function of the relative crack depth (a_1/W).

3.2.2 Forced Vibration

If the cantilever beam with transverse crack is excited at its free end by a harmonic excitation ($Y = Y_0 \sin(\omega t)$), the non-dimensional amplitude at the free end may be expressed as $\bar{y}_2(1) = \frac{Y_0}{L} = \bar{y}_0$. Therefore the boundary conditions for the beam remain same as before except the boundary condition $\bar{y}_2'''(1) = 0$ which modified as $\bar{y}_2(1) = \bar{y}_0$

The constants A_i , $i=1$, to 12 are then computed from the algebraic condition

$$Q_1 D = B_1 \tag{3.14}$$

Q_1 is the (12 x 12) matrix obtained from boundary conditions as mentioned above,

D is a column matrix obtained from the constants,

B_1 is a column matrix, transpose of which is given by, $B_1^T = [0 \ 0 \ 0 \ \bar{y}_0 \ 0 \ 0 \ 0 \ 0 \ 0 \ 0 \ 0 \ 0]$

Chapter 4

Fuzzy Controller Analysis

4. Fuzzy Controller Analysis

4.1 Introduction

The term fuzzy logic has been used in two different senses. It thus important to clarify the distinctions between these two different usages of the term. In a narrow sence, fuzzy logic refers to a logical system that generalizes classical two-valued logic for reasoning under uncertainty. In a broad sense, fuzzy logic refers to all of the theories and technology that employ fuzzy sets, which are classes with unsharp boundaries as referred by Yen and Lengari [50].

4.2 Fuzzy Set Theory

The idea of fuzzy sets was born in July 1964 by Lofti A. Zadeh who made significant contribution in the development of system theory (e.g., the state variable approach to the solution of simultaneous differential equations) and computer science. A fuzzy set is a set with smooth boundary. Fuzzy set theory generalizes classical set theory to allow partial membership. The best way to introduce fuzzy set is to start with a limitation of classical sets.

4.3 Membership Function

A fuzzy set is defined by a function that maps objects in a domain of concern to their membership value in the set. Such a function is known as “membership function”. It is usually denoted by the Greek symbol μ for ease of the recognition and consistency. In other words membership function can be defined as a curve that defines how each point in the input space is mapped to a membership value (or degree of membership) between 0 and 1. The input space is sometimes referred to as the universe of discourse, a fancy name for a simple concept.

4.3.1. Membership functions in Fuzzy Logic-Tool Box

The only condition a membership function must really satisfy is that it must vary between 0 and 1. The function itself can be an arbitrary curve whose shape we can define as a function that suits us from the point of view of simplicity, convenience, speed, and efficiency.

A classical set might be expressed as

$$A = \{x \mid x > 6\}$$

A fuzzy set is an extension of a classical set. If X is the universe of discourse and its elements are denoted by x , then a fuzzy set A in X is defined as a set of ordered pairs.

$$A = \{x, \mu_A(x) \mid x \in X\}$$

$\mu_A(x)$ is called the membership function (or MF) of x in A . The membership function maps each element of X to a membership value between 0 and 1.

The toolbox includes 11 built-in membership function types. These 11 functions are, in turn, built from several basic functions:

1. piecewise linear functions
2. the Gaussian distribution function
3. the sigmoid curve
4. quadratic and cubic polynomial curves

The simplest membership functions are formed using straight lines. Of these, the simplest is the triangular membership function, and it has the function name *trimf*. This function is nothing more than a collection of three points forming a triangle. The trapezoidal membership function, *trapmf*, has a flat top and really is just a truncated triangle curve. These straight line membership functions have the advantage of simplicity. Two membership functions are built on the Gaussian distribution curve: a simple Gaussian curve and a two-sided composite of two different Gaussian curves. The two functions are known as *gaussmf* and *gauss2mf*. The syntax used for Gaussian membership function is:

$$y = \text{gaussmf}(x, [\text{sig } c])$$

The symmetric Gaussian function depends on two parameters and c as given by

$$f(x; \sigma, c) = e^{-\frac{(x-c)^2}{2\sigma^2}},$$

where the parameters for *gaussmf* represent the parameters and c

listed in order in the vector `[sig c]`.

4.4. Linguistic Variables

A linguistic variable enables its value to be described both qualitatively by a linguistic term (i.e., a symbol serving as the name of a fuzzy set) and quantitatively by a corresponding membership function (which expresses the meaning of the fuzzy set). The linguistic term is used to express concepts and knowledge in human communication, whereas membership function is useful for processing numeric input data.

4.5. Fuzzy Rules

Among all the techniques developed using fuzzy sets, the fuzzy if-then rule (or, in short, the fuzzy rule) is by far the most visible one due to its wide range successful applications. Fuzzy if-then rules have been applied to various disciplines such as control systems, decision making, pattern recognition, system modeling and last but not the least in Vibration applications.

Fuzzy sets and fuzzy operators are the subjects and verbs of fuzzy logic. These if-then rule statements are used to formulate the conditional statements that comprise fuzzy logic. A single fuzzy if-then rule assumes the form “if x is A then y is B ”. Where A and B are linguistic values defined by fuzzy sets on the ranges (universes of discourse) X and Y , respectively. The if-part of the rule " x is A " is called the antecedent or premise, while the then-part of the rule " y is B " is called the consequent or conclusion. An example of such a rule might be “if service is good then tip is average”. The concept good is represented as a number between 0 and 1, and so the antecedent is an interpretation that returns a single number between 0 and 1. Conversely, average is represented as a fuzzy set, and so the consequent is an assignment that assigns the entire fuzzy set B to the output variable y . In the if-then rule, the word is gets used in two entirely different ways depending on whether it appears in the antecedent or the consequent. In MATLAB® terms, this usage is the distinction between a relational test using "==" and a variable assignment using the "=" symbol. A less confusing way of writing the rule would be “If service == good then tip = average”. In general, the input to an if-then rule is the current value for the input variable (in this case, service) and the output is an entire fuzzy set (in this case, average). This set will later be defuzzified, assigning one value to the output. The concept of defuzzification is described in the next section. Interpreting an if-then rule

involves distinct parts: first evaluating the antecedent (which involves fuzzifying the input and applying any necessary fuzzy operators) and second applying that result to the consequent (known as implication). In the case of two-valued or binary logic, if-then rules do not present much difficulty. If the premise is true, then the conclusion is true. If you relax the restrictions of two-valued logic and let the antecedent be a fuzzy statement, how does this reflect on the conclusion? The answer is a simple one. if the antecedent is true to some degree of membership, then the consequent is also true to that same degree.

4.6. Fuzzy Controller Analysis for the Crack localization and Identification.

The fuzzy controller has been developed where there are 3 inputs and 2 outputs parameter. The natural linguistic representations for the input are as follows

Relative first natural frequency = “FNF”

Relative second natural frequency = “SNF”

Relative third natural frequency = “TNF”

The natural linguistic term used for the outputs are

Relative crack depth = “RCD”

Relative crack length= “RCL”

The membership functions names for the linguistic terms, as shown in the figure 4.1. Figure 4.1 (a) shows the various linguistic terms used for the Relative 1st mode natural frequency. It has total 10 number of membership functions. Similarly Figure 4.1 (b) and 4.1 (c) show the membership functions and the respective linguistic terms used for 2nd and 3rd mode relative natural frequencies. And both are having 10 membership functions each.

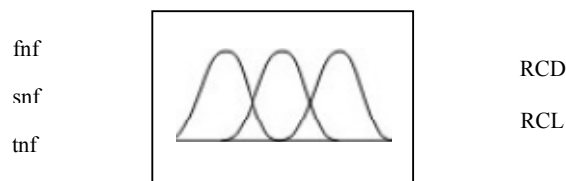


Fig. 4.1 Membership Functions shown in the Fuzzy Controller

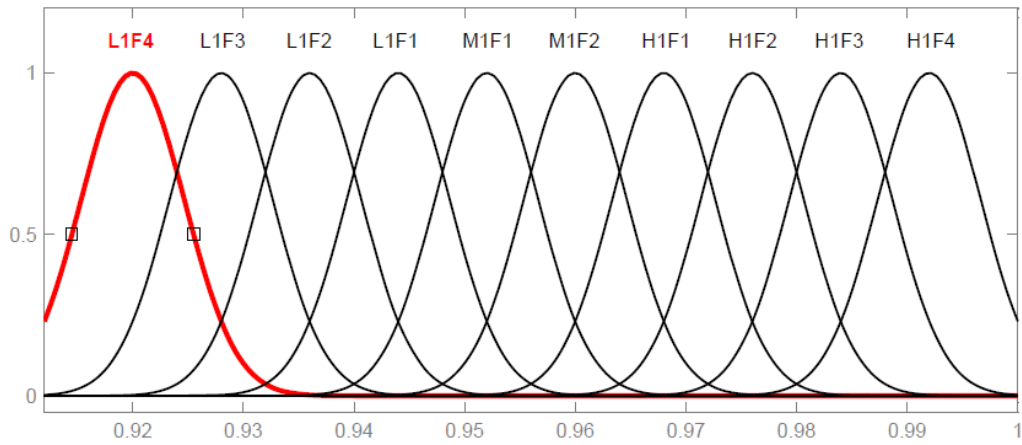


Fig: 4.1 (a) Membership functions for relative natural frequency for 1st Mode of Vibration

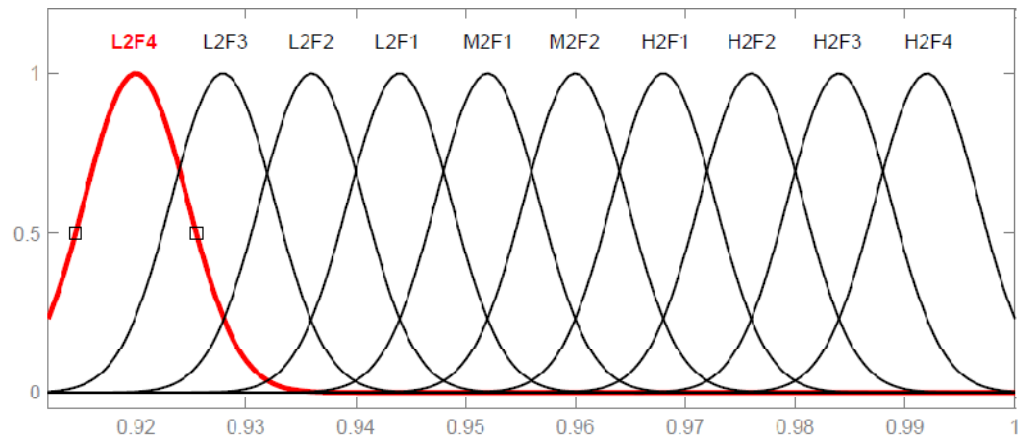


Fig: 4.1 (b) Membership functions for relative natural frequency for 2nd Mode of Vibration

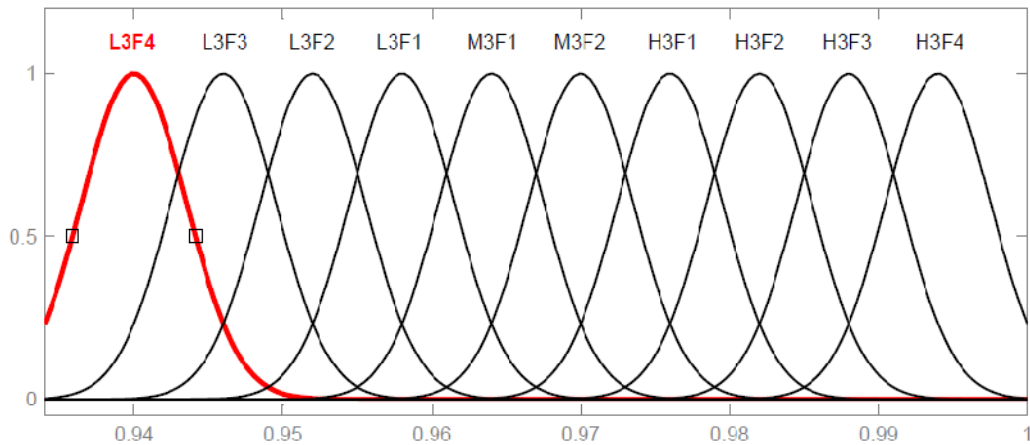


Fig: 4.1 (c) Membership functions for relative natural frequency for 3rd Mode of Vibration

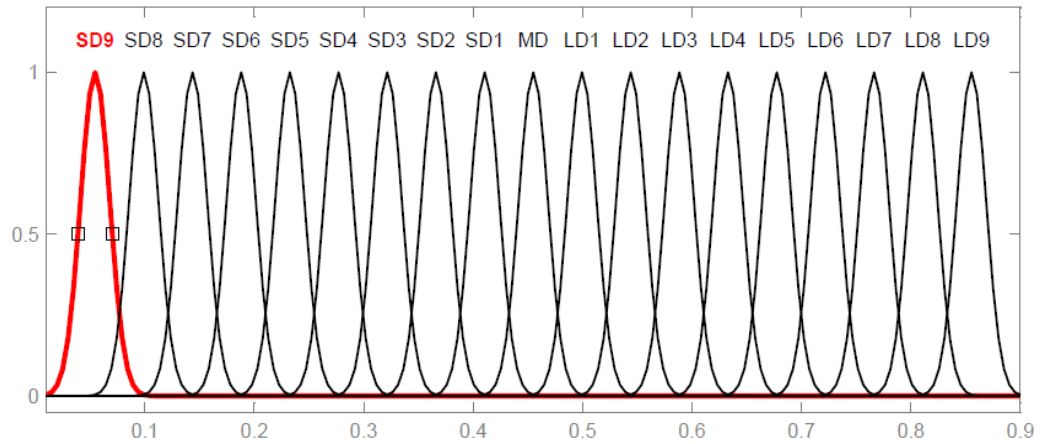


Fig: 4.1 (d) Membership functions for crack depth

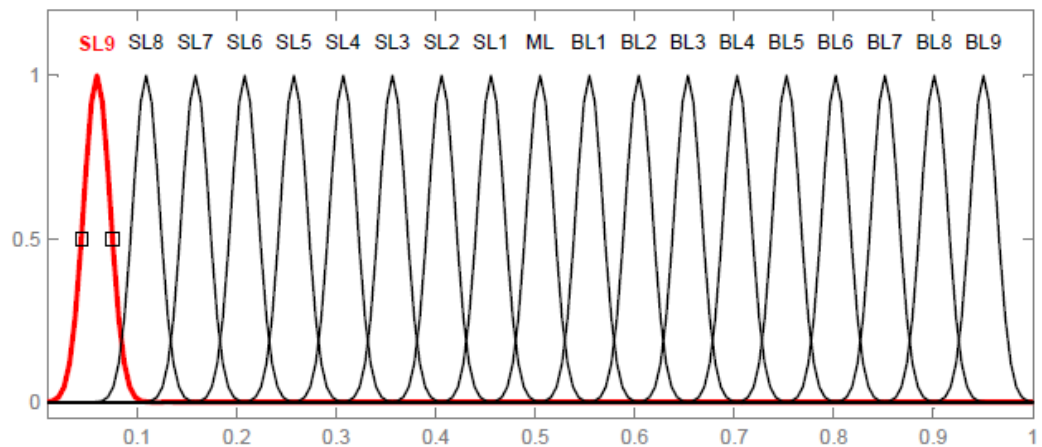


Fig: 4.1 (e) Membership functions for crack length

The linguistic terms used in the Fuzzy Interference system are as described in a tabular form in Table 4.1.

Table 4.1 Fuzzy Linguistic Terms used

Name of the Membership function	Linguistic terms	Description and range of the linguistic terms
L1F1,L1F2,L1F3,L1F4	$fnf_{1\ to\ 4}$	Low ranges of relative natural frequency for first mode of vibration in descending order respectively
M1F1, M1F2	$fnf_{5,6}$	Medium ranges of relative natural frequency for first mode of vibration in ascending order respectively
H1F1,H1F2,H1F3,H1F4	$fnf_{7\ to\ 10}$	Higher ranges of relative natural frequency for first mode of vibration in ascending order respectively
L2F1,L2F2,L2F3,L2F4	$snf_{1\ to\ 4}$	Low ranges of relative natural frequency for second mode of vibration in descending order respectively
M2F1, M2F2	$snf_{5,6}$	Medium ranges of relative natural frequency for second mode of vibration in ascending order respectively
H2F1,H2F2,H2F3,H2F4	$snf_{7\ to\ 10}$	Higher ranges of relative natural frequencies for second mode of vibration in ascending order respectively
L3F1,L3F2,L3F3,L3F4	$tnf_{1\ to\ 4}$	Low ranges of relative natural frequencies for third mode of vibration in descending order respectively
M3F1.M3F2	$tnf_{5,6}$	Medium ranges of relative natural frequencies for third mode of vibration in ascending order respectively
H3F1,H3F2,H3F3,H3F4	$tnf_{7\ to\ 10}$	Higher ranges of relative natural frequencies for third mode of vibration in ascending order respectively
SD1,SD2,.....SD9	$rcd_{1\ to\ 9}$	Small ranges of relative crack depth in

MD	rcd ₁₀	descending order respectively Medium relative crack depth
LD1,LD2.....LD9	rcd _{11 to 19}	Larger ranges of relative crack depth in ascending order respectively
SL1.SL2.....SL9	rcl _{1 to 9}	Small ranges of relative crack location in descending order respectively
ML	rcl ₁₀	Medium relative crack length
BL1,BL2.....BL9	rcl _{11 to 19}	Bigger ranges of relative crack location in ascending order respectively

4.7 Fuzzy mechanism used for crack detection

Based on the above fuzzy subset the fuzzy rules are defined in a general form as follows:

If (FNF is FNF_i and SNF is SNF_j and TNF is TNF_k) then (CD is CD_{ijk} and CL is CL_{ijk})

Where i= 1to 10, j=1 to 10, k=1 to 10 (4.1)

Because of “FNF”, “SNF”, “TNF” have 10 membership functions each.

From the above expression (14), two set of rules can be written

If (FNF is FNF_i and SNF is SNF_j and TNF is TNF_k) then CD is CD_{ijk} }
 If (FNF is FNF_i and SNF is SNF_j and TNF is TNF_k) then CL is CL_{ijk} } (4.2)

According to the usual Fuzzy logic control method (Parhi, 2005), a factor W_{ijk} is defined for the rules as follows:

$$W_{ijk} = \mu_{fnf_i}(\text{freq}_i) \wedge \mu_{snf_j}(\text{freq}_j) \wedge \mu_{tnf_k}(\text{freq}_k)$$

Where freq_i , freq_j and freq_k are the first, second and third natural frequency of the cantilever beam with crack respectively ; by Applying composition rule of interference (Parhi, 2005) the membership values of the relative crack location and relative crack depth (location)_{CL}

$$\mu_{\text{rcl}_{ijk}}(\text{location}) = W_{ijk} \wedge \mu_{\text{rcl}_{ijk}}(\text{location}) \quad \forall \text{length} \in \text{CL}$$

As;

$$\mu_{\text{rcl}_{ijk}}(\text{depth}) = W_{ijk} \wedge \mu_{\text{rcl}_{ijk}}(\text{depth}) \quad \forall \text{depth} \in \text{CD}$$

The overall conclusion by combining the output of all the fuzzy can be written as follows:

$$\left. \begin{aligned} \mu_{\text{rcl}_{ijk}}(\text{location}) &= \mu_{\text{rcl}_{111111}}(\text{location}) \vee \dots \vee \mu_{\text{rcl}_{ijk}}(\text{location}) \\ \vee \vee \mu_{\text{rcl}_{19\ 19\ 19\ 19\ 19}}(\text{location}) \\ \mu_{\text{rcl}_{ijk}}(\text{location}) &= \mu_{\text{rcl}_{111111}}(\text{depth}) \vee \dots \vee \mu_{\text{rcl}_{ijk}}(\text{depth}) \\ \vee \dots \vee \mu_{\text{rcl}_{19\ 19\ 19\ 19\ 19}}(\text{depth}) \end{aligned} \right\} \quad (4.3)$$

The crisp values of relative crack location and relative crack depth are computed using the center of gravity method (Parhi, 2005) as:

$$\left. \begin{aligned} \text{Relative crack location} = \text{RCL} &= \frac{\int \text{location} \cdot \mu_{\text{rcl}}(\text{location}) \cdot d(\text{location})}{\int \mu_{\text{rcl}}(\text{location}) \cdot d(\text{location})} \\ \text{Relative crack depth} = \text{RCD} &= \frac{\int \text{depth} \cdot \mu_{\text{rcl}}(\text{depth}) \cdot d(\text{depth})}{\int \mu_{\text{rcl}}(\text{depth}) \cdot d(\text{depth})} \end{aligned} \right\} \quad (4.4)$$

4.8 Output (Crack Length and crack Depth) using Fuzzy Controller

The inputs to the fuzzy controller are relative first mode natural frequency (FNF); relative second mode frequency (SNF) and relative third mode natural frequency (TNF). The outputs from the fuzzy controller are relative crack depth (RCD) and relative crack location (RCL). A few numbers of rules out of several hundred fuzzy rules are being enlisted in the Table 4.2. Figure 4.2 shows the fuzzy controller results when rule-8 and rule-20 are activated from Table 4.2.

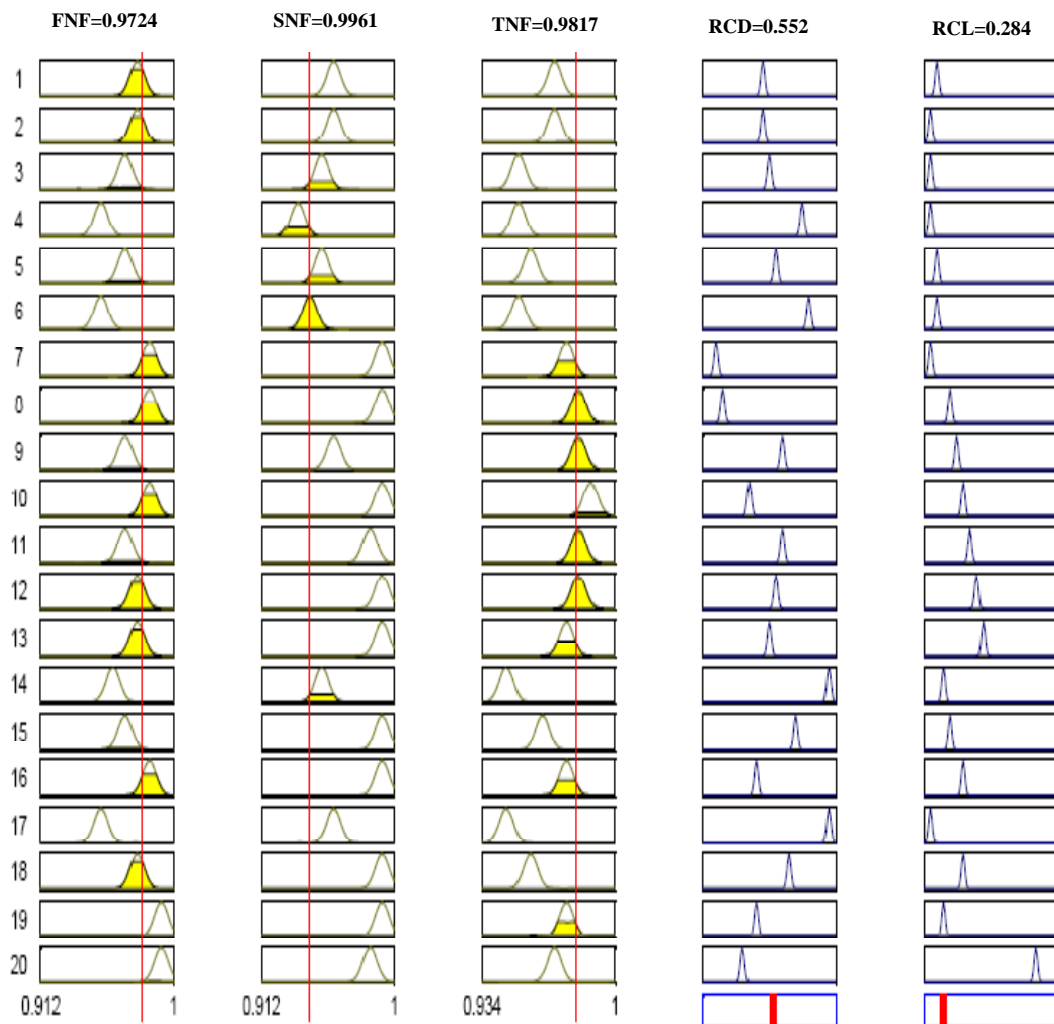


Fig. 4.2 Resultant values of relative crack depth and relative crack location when Rule 20 are activated

Table 4.2 Example of some fuzzy rules used in the Fuzzy Controller

Sl No.	Example of some of the few rules used in the Fuzzy Controller
1	If fnf is H1F2,snf is M2F2,tnf is M3F2, then rcd is SD1,and rcl is SL8
2	If fnf is H1F2,snf is M2F2,tnf is M3F2, then rcd is SD1,and rcl is SL9
3	If fnf is H1F1,snf is M2F1,tnf is L3F2, then rcd is MD, and rcl is SL9
4	If fnf is M1F1,snf is L2F2,tnf is L3F2, then rcd is LD5,and rcl is SL9
5	If fnf is H1F1,snf is M2F1,tnf is L3F1, then rcd is LD1,and rcl is SL8
6	If fnf is M1F1,snf is L2F1,tnf is L3F2, then rcd is LD6,and rcl is SL8
7	If fnf is H1F3,snf is H2F4,tnf is H3F1, then rcd is SD8,and rcl is SL9
8	If fnf is H1F3,snf is H2F4,tnf is H3F2, then rcd is SD7,and rcl is SL6
9	If fnf is H1F1,snf is M2F2,tnf is H3F2, then rcd is SD3,and rcl is SL4
10	If fnf is H1F3,snf is H2F4,tnf is H3F4, then rcd is SD3,and rcl is SL4
11	If fnf is H1F1,snf is H2F3,tnf is H3F2, then rcd is LD1,and rcl is SL3
12	If fnf is H1F2,snf is H2F4,tnf is H3F2, then rcd is LD1,and rcl is SL2
13	If fnf is H1F2,snf is H2F4,tnf is H3F1, then rcd is MD, and rcl is SL1
14	If fnf is M1F2,snf is M2F1,tnf is L3F4, then rcd is LD9,and rcl is SL7
15	If fnf is H1F1,snf is H2F4,tnf is M3F1, then rcd is LD4,and rcl is SL6
16	If fnf is H1F3,snf is H2F4,tnf is H3F1, then rcd is SD2,and rcl is SL4
17	If fnf is M1F1,snf is M2F2,tnf is L3F3, then rcd is LD9,and rcl is SL9
18	If fnf is H1F2,snf is H2F4,tnf is L3F1, then rcd is LD3,and rcl is SL4
19	If fnf is H1F4,snf is H2F4,tnf is H3F1, then rcd is SD2,and rcl is SL7
20	If fnf is H1F4,snf is H2F3,tnf is M3F2, then rcd is SD4,and rcl is BL7

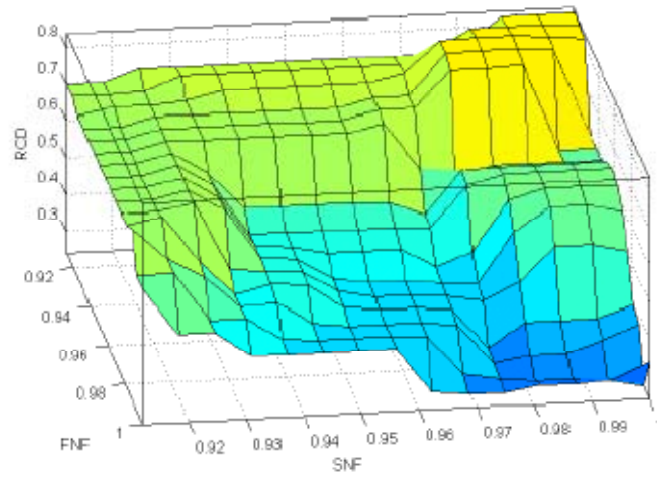


Fig. 4.3 Surface view of relative first and second natural frequency with relative crack depth

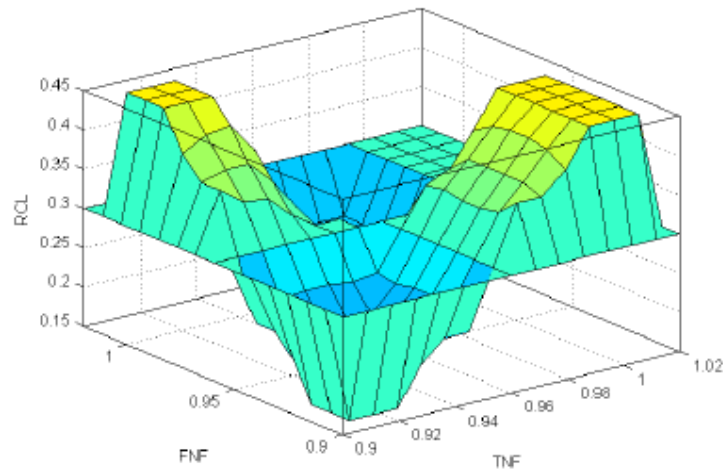


Fig. 4.4 Surface view of relative first and third natural frequency with relative crack length

Chapter 5

Finite Element Formulation

5. Finite Element Formulation

5.1 Theory

The beam with a transverse edge crack is clamped at left end, free at right end and has uniform structure with a constant rectangular cross-section of 800 mm X 50 mm X 6 mm. The Euler-Bernoulli beam model is assumed for the finite element formulation. The crack in this particular case is assumed to be an open crack and the damping is not being considered in this theory. Both single and double edged crack are considered for the formulation.

5.2 Governing Equation of Free Vibration

The free bending vibration of an Euler-Bernoulli beam of a constant rectangular cross-section is given by the following differential equation as given in:

$$EI \frac{d^4 y}{dx^4} - m\omega_i^2 y = 0 \quad (5.1)$$

Where m is the mass of the beam per unit length (kg/m), ω_i is the natural frequency of the i th mode (rad/sec), E is the modulus of elasticity (N/m²) and I is the moment of inertia (m⁴). By defining $\lambda^4 = \omega_i^2 m / EI$ equation (5.1) is rearranged as a fourth-order differential equation as follows:

$$\frac{d^4 y}{dx^4} - \lambda^4 y = 0 \quad (5.2)$$

The general solution to equation (5.2) is

$$y = A \cos \lambda_i x + B \sin \lambda_i x + C \cosh \lambda_i x + D \sinh \lambda_i x \quad (5.3)$$

Where A , B , C , D are constants and λ_i is a frequency parameter. Since the bending vibration is studied, edge crack is modeled as a rotational spring with a lumped stiffness. The crack is assumed open. Based on this modeling, the beam is divided into two segments: the first and second segments are left and right-hand side of the crack, respectively. Adopting Hermitian shape functions, the stiffness matrix of the two-noded beam element without a crack is obtained using the standard integration based on the variation in flexural rigidity as

$$[K^e] = \int [B(x)]^T EI [B(x)] dx \quad (5.4)$$

$$\text{Where } [B(x)] = \{H_1''(x)H_2''(x)H_3''(x)H_4''(x)\}, \quad (5.5)$$

And $H_1(x), H_2(x), H_3(x), H_4(x)$ are the Hermitian shape functions defined as

$$H_1(x) = 1 - \frac{3x^2}{l^2} + \frac{2x^3}{l^3} \quad (5.5a)$$

$$H_2(x) = x - \frac{2x^2}{l} + \frac{x^3}{l^2} \quad (5.5b)$$

$$H_3(x) = \frac{3x^2}{l^2} - \frac{2x^3}{l^3} \quad (5.5c)$$

$$H_4(x) = -\frac{2x^2}{l} + \frac{x^3}{l^2} \quad (5.5d)$$

Assuming the beam rigidity EI is constant and is given by EI_0 within the element, and then the element stiffness is

$$[K^e] = \frac{EI_0}{l^3} \begin{bmatrix} 12 & 6l & -12 & 6l \\ 6l & 4l^2 & -6l & 2l^2 \\ -12 & -6l & 12 & -6l \\ 6l & 2l^2 & -6l & 4l^2 \end{bmatrix} \quad (5.6)$$

Assuming the stiffness reduction caused by an open crack falls within a single element, and then the stiffness matrix $[K_c^e]$ of the cracked element can be written as

$$[K_c^e] = [K^e] - [K_c] \quad (5.7)$$

Where $[K_c]$ is the reduction in the stiffness matrix due to the crack. According to Peng et al. [17], the matrix $[K_c]$ is

$$[K_c] = \begin{bmatrix} k_{11} & k_{12} & -k_{11} & k_{14} \\ k_{12} & k_{22} & -k_{12} & k_{24} \\ -k_{11} & -k_{12} & k_{11} & -k_{14} \\ k_{14} & k_{24} & -k_{14} & k_{44} \end{bmatrix} \quad (5.8)$$

Where

$$k_{11} = \frac{12E(I_0 - I_c)}{l^4} \left[\frac{2l_c^2}{l^2} + 3l_c \left(\frac{2\xi}{l^2} - 1 \right)^2 \right] \quad (5.8a)$$

$$k_{12} = \frac{12E(I_0 - I_c)}{l^3} \left[\frac{l_c^3}{l^2} + l_c \left(2 - \frac{7\xi}{l} + \frac{6\xi^2}{l^2} \right) \right] \quad (5.8b)$$

$$k_{14} = \frac{12E(I_0 - I_c)}{l^3} \left[\frac{l_c^3}{l^2} + l_c \left(1 - \frac{5\xi}{l} + \frac{6\xi^2}{l^2} \right) \right] \quad (5.8c)$$

$$k_{22} = \frac{12E(I_0 - I_c)}{l^2} \left[\frac{3l_c^2}{l^2} + 2l_c \left(\frac{3\xi}{l} - 2 \right)^2 \right] \quad (5.8d)$$

$$k_{24} = \frac{12E(I_0 - I_c)}{l^2} \left[\frac{3l_c^2}{l^2} + 2l_c \left(2 - \frac{9\xi}{l} + \frac{9\xi^2}{l^2} \right)^2 \right] \quad (5.8e)$$

$$k_{44} = \frac{12E(I_0 - I_c)}{l^2} \left[\frac{3l_c^2}{l^2} + 2l_c \left(\frac{3\xi}{l} - 1 \right)^2 \right] \quad (5.8f)$$

$l_c = 1.5d$, and ξ is the distance between the left node and the crack as shown in Figure 5.3. It is supposed that the crack does not affect the mass distribution of the beam. Therefore, the consistent mass matrix of the beam element can be formulated directly as

$$[M^e] = \int_0^l \rho A [H(x)]^T [H(x)] \quad (5.9)$$

$$\text{And we have } [M^e] = \frac{\rho A l}{420} \begin{bmatrix} 156 & 22l & 54 & -13l \\ 22l & 4l^2 & 13l & -3l^2 \\ 54 & 13l & 156 & -22l \\ -13l & -3l^2 & -22l & 4l^2 \end{bmatrix} \quad (5.10)$$

Where $[H(x)] = \{H_1(x)H_2(x)H_3(x)H_4(x)\}$. In the dynamic analysis, the system matrix is usually required to be inverted. From this aspect, a diagonalized mass matrix has a computational advantage. In this study, a diagonalized mass matrix is adopted, which is developed from the consistent mass matrix using the approach

$$[M^e] = \frac{\rho A l}{78} \begin{bmatrix} 39 & 0 & 0 & 0 \\ 0 & l^2 & 0 & 0 \\ 0 & 0 & 39 & 0 \\ 0 & 0 & 0 & l^2 \end{bmatrix} \quad (5.11)$$

The natural frequency then can be calculated from the relation

$$-w^2 [M] + [K] \{\bar{q}\} = 0 \quad (5.12)$$

The natural frequency of the i th mode for uncracked and cracked beams is finally obtained as follows

$$w_{i0} = c_i \sqrt{\frac{EI}{ml^4}} \quad (5.13)$$

$$w_i = r_i c_i \sqrt{\frac{EI}{ml^4}} \quad (5.14)$$

Where w_{i0} is the i th mode frequency of the uncracked beam and c_i is a constant depending on the mode number and beam end conditions (for clamped-free beam, c_i is 3.516 and 22.034 for the first and second mode, respectively), w_i is the i th mode frequency of the cracked beam. r_i is the ratio between the natural frequencies of the cracked and uncracked beam. l is the length of the beam.

5.3 Governing Equation of Forced Vibration

The Euler-Bernoulli beam is discretized into finite beam element without crack and can be written as

$$[M]^{(e)} \left\{ \ddot{q}(t) \right\}^{(e)} + [K_{wc}]^{(e)} \{q(t)\}^{(e)} = \{F(t)\}^{(e)} \quad (5.15)$$

Where $[M]^{(e)}$ is the element mass matrix, $[K_{wc}]^{(e)}$ is the element stiffness matrix, $\{F(t)\}^{(e)}$ is the element external force vector, $\{q(t)\}^{(e)}$ is the element vector of nodal degree of freedom and t is the time instant. The subscript 'wc' represents without crack. And the subscript 'e' represents element and the dot represents the derivative with

respect to the time. The crack is assumed to affect only the stiffness. So the equation of a cracked beam element can be expressed as

$$[M]^{(e)} \left\{ \ddot{q}_c(t) \right\}^{(e)} + [K_c]^{(e)} \{q_c(t)\}^{(e)} = \{F(t)\}^{(e)} \quad (5.16)$$

Where $\{q_c(t)\}^{(e)}$ is the nodal degree of freedom of the cracked element, the subscript 'c' represent the crack and $[K_c]^{(e)}$ is the stiffness matrix of the cracked element and is given as

$$[K_c]^{(e)} = [T][C]^{(e)-1} [T]^T \quad (5.17)$$

With

$$[C]^{(e)} = [C_0]^{(e)} + [C_c]^{(e)} \quad (5.18)$$

Where $[C_0]^{(e)}$ is the flexibility matrix of the uncracked beam element, $[C_c]^{(e)}$ is the flexibility matrix of the crack, and $[C]^{(e)}$ is the total flexibility matrix of the cracked beam element. Equations of motion of the complete system can be obtained by assembling the contribution of all equations of motions motion for cracked and uncracked elements in the system. Then the system equation of motion becomes

$$[M] \left\{ \ddot{q}(t) \right\} + [K] \{q(t)\} = \{F(t)\} \quad (5.19)$$

Where $[M]$ is the assembled mass matrix, $[K]$ is the assembled stiffness matrix, $\{F(t)\}$ is the assembled external force vector, and $\{q(t)\}$ is the assembled vector of nodal degrees of freedom of the system.

Let the force vector be defined as

$$\{F(t)\} = \{\bar{F}\} e^{j\omega t} \quad (5.20)$$

Where ω is the forcing frequency, $\{\bar{F}\}$ is the force amplitude vector (elements of which are complex quantities) and $j = \sqrt{-1}$. Thus, the response vector can be assumed as

$$\{q(t)\} = \{\bar{q}\} e^{j\omega t} \quad (5.21)$$

Where $\{\bar{q}\}$ is the response amplitude vector and their elements are complex quantities. Substituting the equations (5.20) and (5.21) into equation (5.19), the system governing as follows:

$$\left(-\omega^2 [M] + [K]\right)\{\bar{q}\} = \{\bar{F}\} \quad (5.22)$$

For a given system properties (i.e. $[M]$ and $[K]$) the response can be simulated from equation (5.22) corresponding to a given force $\{\bar{F}\}$.

The cracked cantilever beam with double cracks is also analyzed using the above formulation.

5.4 Simulated Crack configuration

In the finite element analysis of the cracked cantilever beam having V-shaped single and double crack is taken into account. The length and cross-sectional area of the beam are 800 mm, and $50 \times 6 \text{ mm}^2$, respectively. As per the material properties the modulus of elasticity (E) is 70 Gpa, the density (ρ) is 2710 kg/m^3 and the Poisson's ratio (μ) is 0.3.

Different crack configurations of same depth and at different locations (from different distance from the fixed end) are prepared to find out how the crack affects the dynamic behavior of the beam. Crack depth was kept constant at 0.202 mm and the crack location from the fixed end was varied at instances of 50 mm, 100 mm, 200 mm, 300 mm, 400 mm, 500 mm, 600 mm and 700 mm. And the effect of crack location on the natural frequencies was investigated. Similarly double edged cracks were formulated on the cantilever beam and the effect was verified. Figures 5.1 to 5.9 show the different crack locations from the fixed end keeping the crack depth fixed.

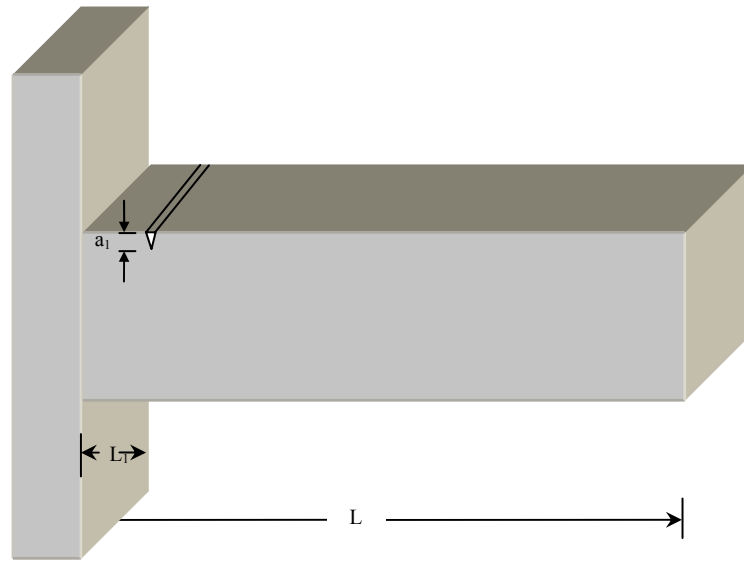


Fig. 5.1 Crack location at $L_1 = 50$ mm and crack depth $a_1 = 0.202$

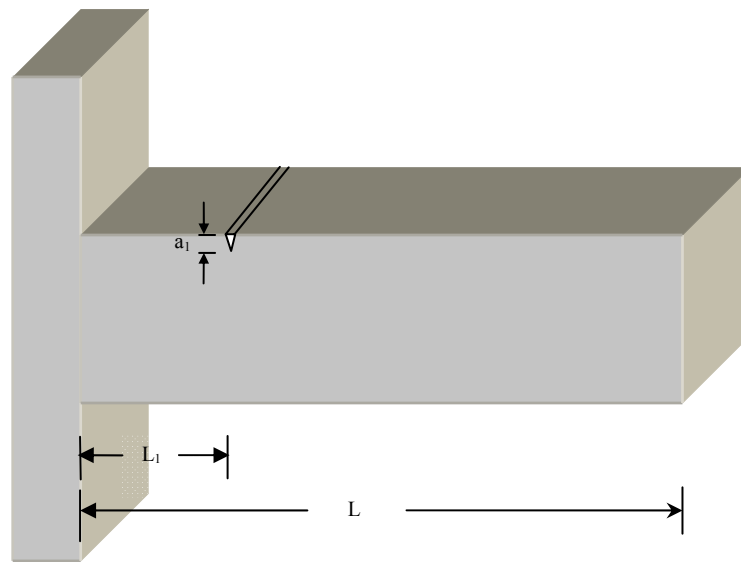


Fig. 5.2 Crack location at $L_1 = 100$ mm and crack depth $a_1 = 0.202$

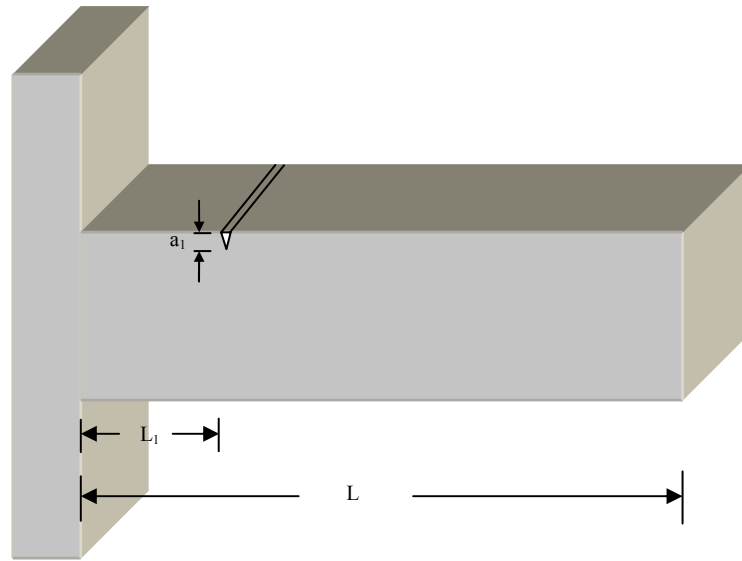


Fig. 5.3 Crack location at $L_1 = 200$ mm and crack depth $a_1 = 0.202$

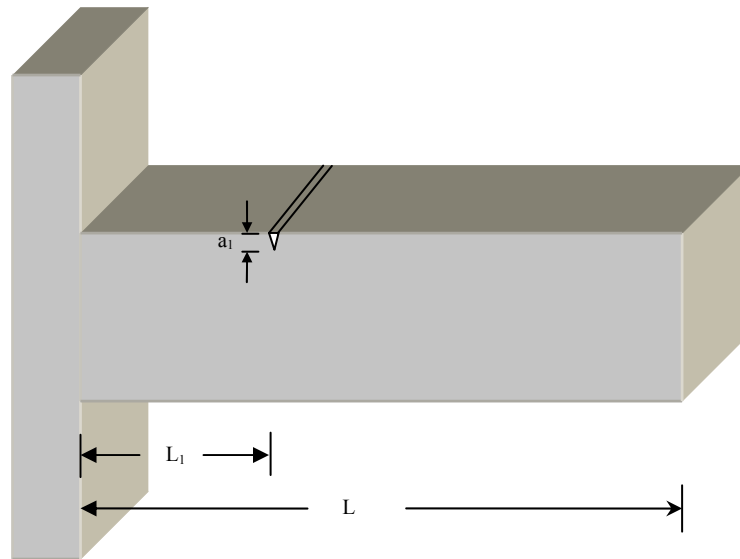


Fig. 5.4 Crack location at $L_1 = 200$ mm and crack depth $a_1 = 0.202$

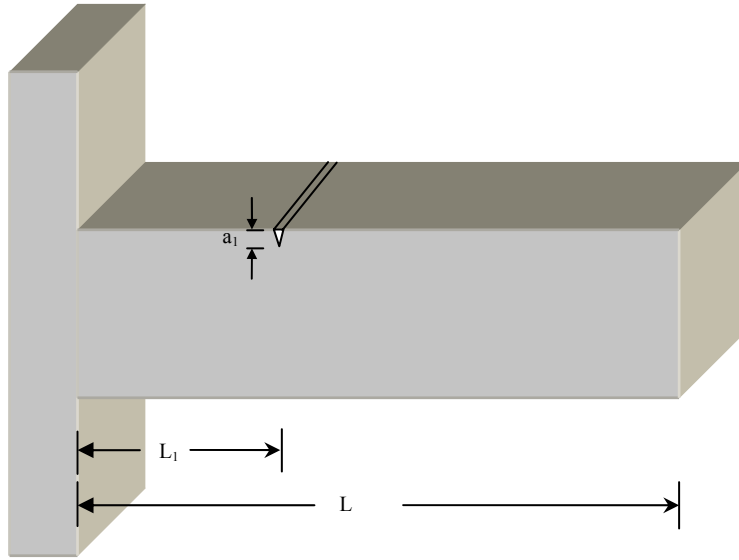


Fig. 5.5 Crack location at $L_1 = 300$ mm and crack depth $a_1 = 0.202$

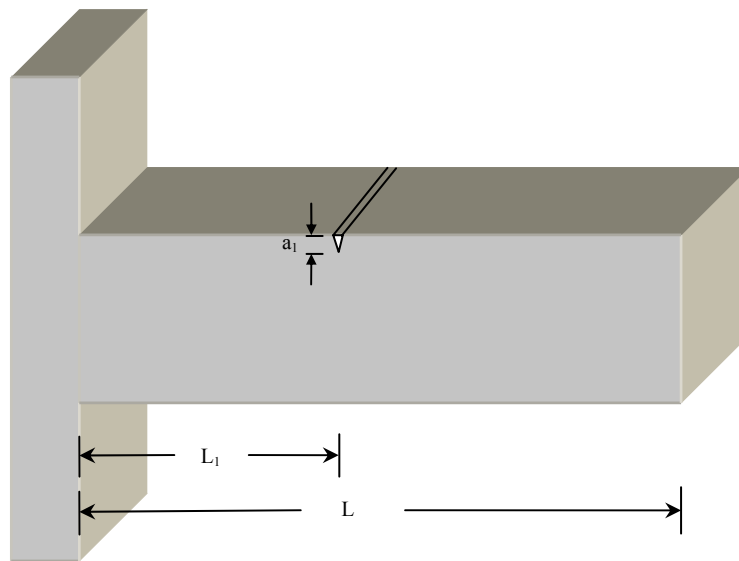


Fig. 5.6 Crack location at $L_1 = 400$ mm and crack depth $a_1 = 0.202$

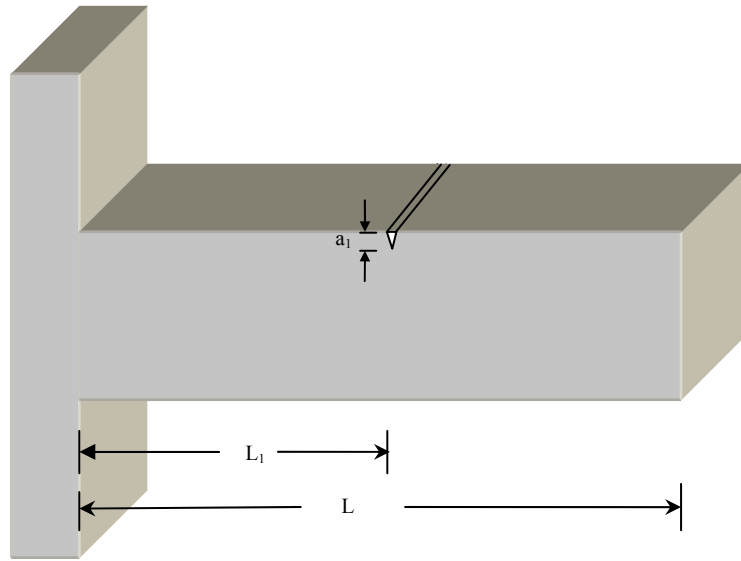


Fig. 5.7 Crack location at $L_1 = 500$ mm and crack depth $a_1 = 0.202$

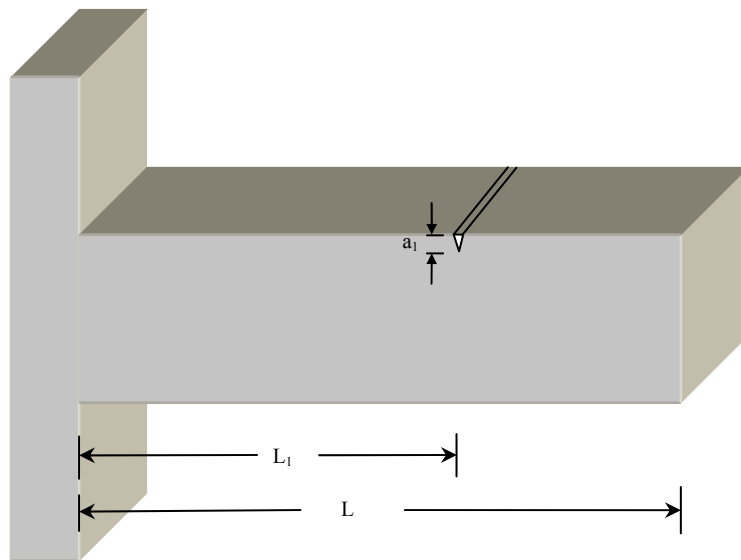


Fig. 5.8 Crack location at $L_1 = 600$ mm and crack depth $a_1 = 0.202$

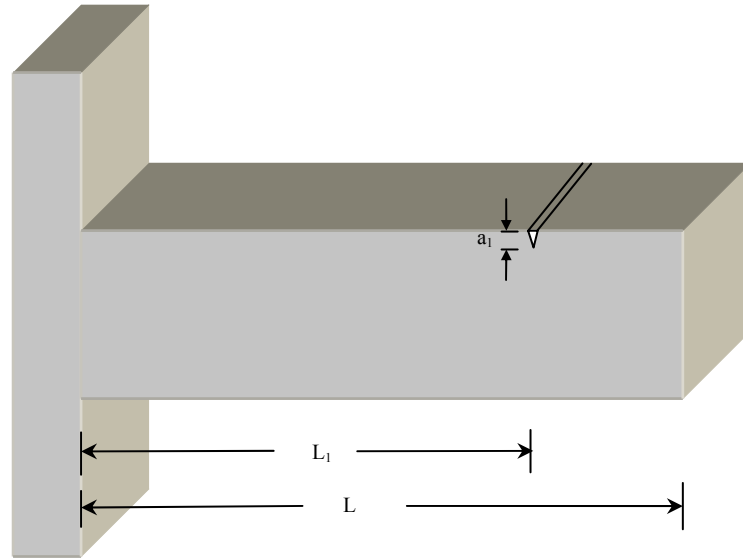


Fig. 5.9 Crack location at $L_1 = 700$ mm and crack depth $a_1 = 0.202$

Similarly double cracks for the cantilever beam were formulated at different crack locations from the fixed end. Out of the several double crack locations the positions of the two transverse crack is as shown in the figure 5.10.

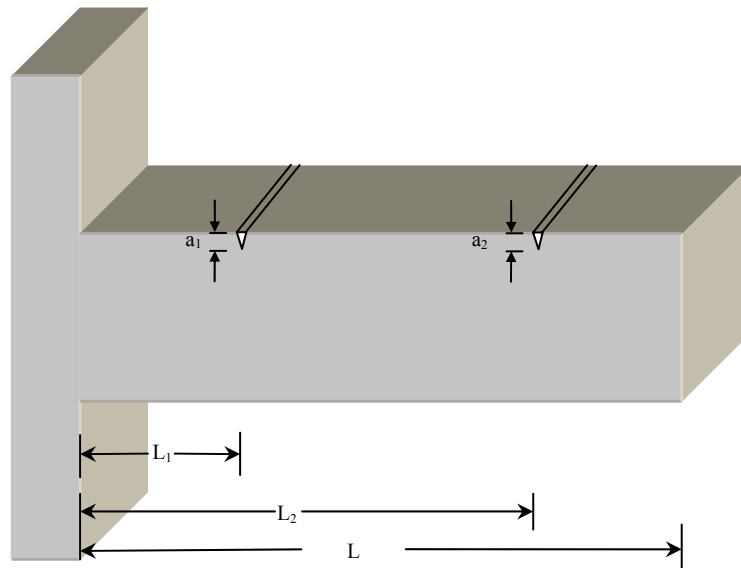


Fig. 5.10 Two Crack location at $L_1 = 100$ mm and $L_2 = 700$ mm with crack depth $a_1 = 0.202$

5.5 Finite Element Modeling

The ALGOR V 19.3 SP 2 Finite Element Program [51] was used for vibration analysis of the uncracked and cracked cantilever beam. For this purpose the beam element with different single and double crack locations were plotted using CATIA V5R15 software. The crack width was taken as 0.202 mm and the crack depth was kept fixed at 0.202 mm. The uncracked and cracked beam model was then analyzed in ALGOR environment. First of all the mesh generation was performed. The mesh size was around 3.333 and approximately 8220 elements with 11568 nodes were created. Then from the tool command FEA model was created by using the FEA editor. Then the parameters such as element type, material name were defined in the ALGOR environment. Then cantilever boundary conditions were modeled by constraining all degrees of freedom of the nodes located on the left end of the beam. The model unit was then changed to S.I. standards. Then in the analysis window the particular analysis type was selected (natural frequency i.e. modal analysis). Then the analysis was performed and the three modes of natural frequencies at different crack locations of the single and double crack cantilever beam were noted down. Figure 5.11 shows the Finite Element modeling of the uncracked cantilever beam in the ALGOR environment. Figure 5.12 shows the finite element modeling of the single cracked beam. And figure 5.13 indicate the details of the crack zone.

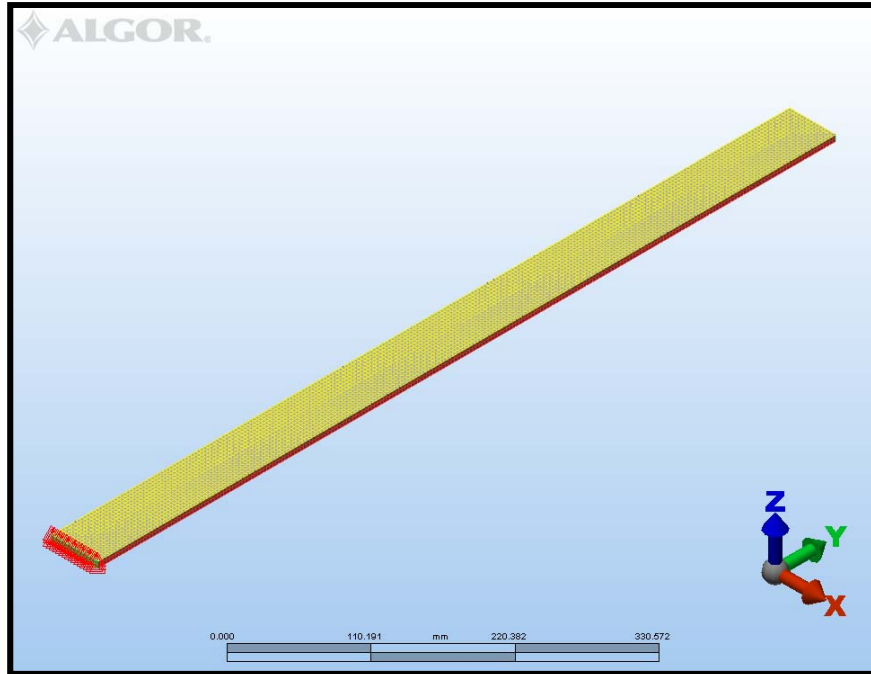


Fig. 5.11 Finite Element modeling of the uncracked cantilever beam in ALGOR

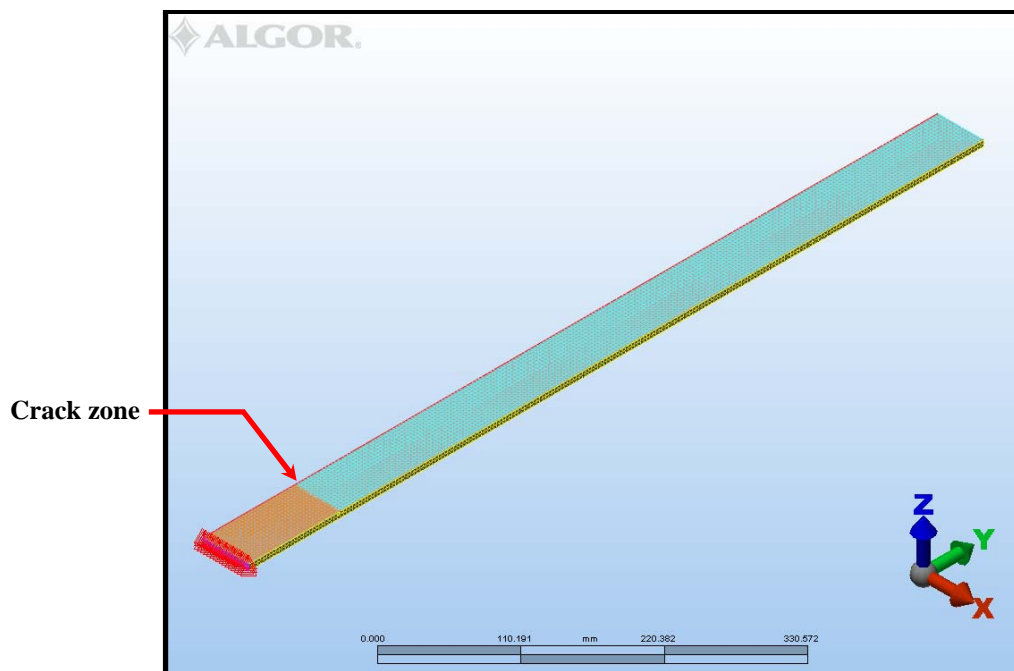


Fig. 5.12 Finite Element modeling of the single-cracked cantilever beam in ALGOR

The Finite Element modeling of the double cracked beam is as shown in figure 5.13

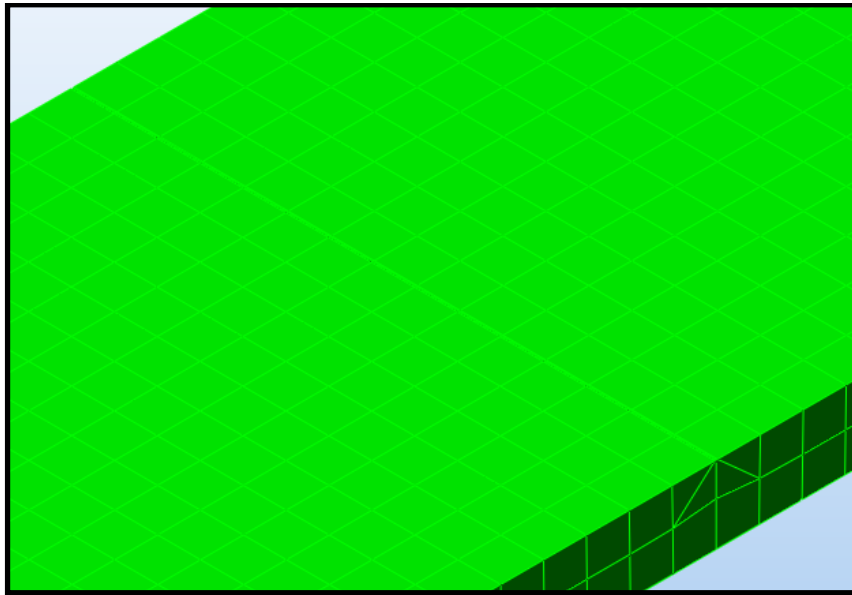


Fig. 5.13 Details of the crack zone in ALGOR

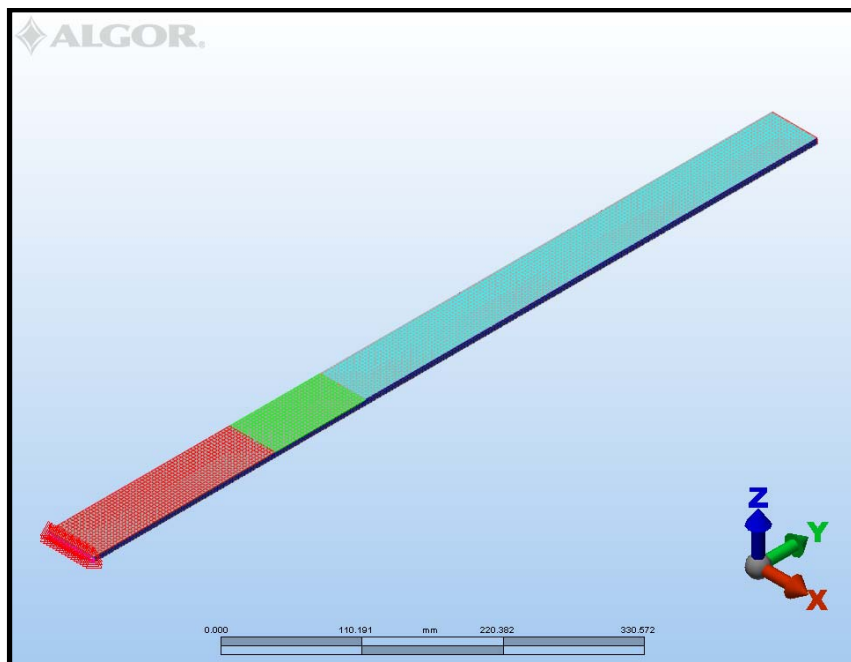


Fig. 5.14 Finite Element modeling of the double-cracked cantilever beam in ALGOR

The modal frequencies of a few of the cracked cantilever beam model generated are as shown in figure 5.15

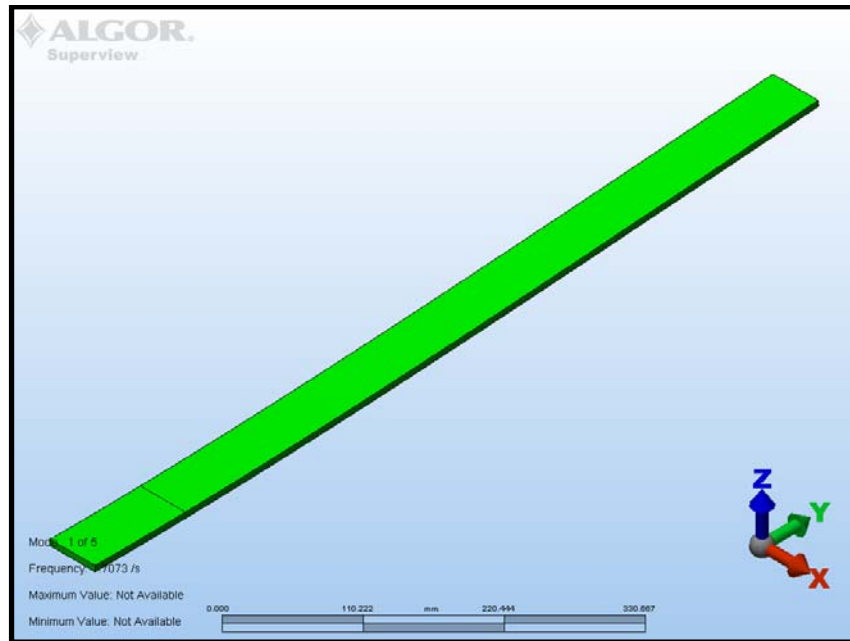


Fig. 5.15 (a) 1st mode frequency of the cracked cantilever beam model

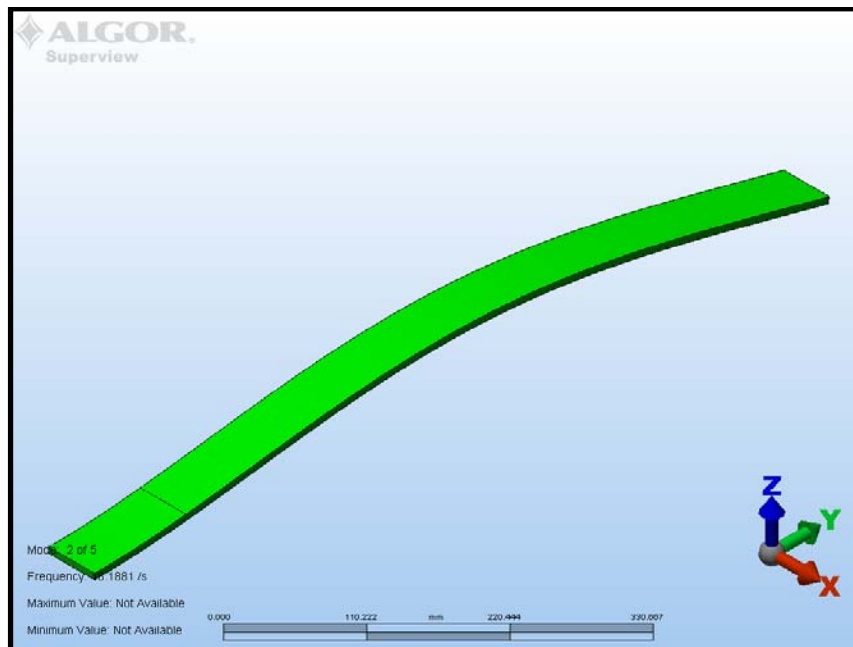


Fig. 5.15 (b) 2nd mode frequency of the cracked cantilever beam model

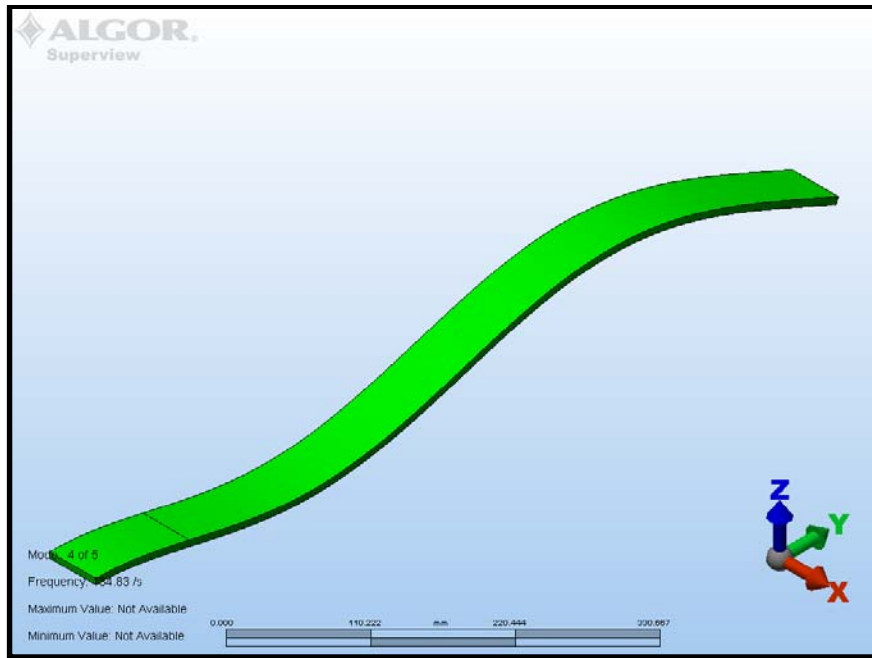


Fig. 5.15 (c) 3rd mode frequency of the cracked cantilever beam model

Chapter 6

Results and Discussions

6. Results and Discussions

6.1 Experimental Set-up

Experimental analysis was performed to find out the three modal natural frequencies of the single and double edged cracked cantilever beam. In the experiments various crack positions (length from the fixed end of the cantilever beam) were given in the cantilever beam. Crack positions were varied from the fixed end with an interval of 50 mm, 100 mm, 200 mm, 300 mm, 400 mm, 500 mm, 600 mm, and 700 mm. For the double edged cracked cantilever beam the positions of V-shaped cracks were placed at 50 mm and 100 mm, 100 mm and 200 mm, 200 mm and 300 mm etc. These results were used to be given as a training data to the Fuzzy Interference System. By incorporating the training data and the fuzzy rules the Fuzzy Controller was able to give outputs in terms of relative crack depth and relative crack lengths with the three inputs of the relative first, second and third modes of modal natural frequencies. The line-diagram of the Experimental set-up for performing the experiments is as shown in figure 6.1. Several tests were conducted on Aluminum cantilever beam specimen with single and double transverse crack. The length of the beam taken as 800 mm and the cross-sectional area was $50 \times 6 \text{ mm}^2$.

6.1 Results

The INSTRON set-up was used to provide the transverse cracks at the desired locations. The specimens of cracked cantilever beams were used to obtain the modal natural frequencies. The modal natural frequencies were then used as a training data and were given as an input to the Fuzzy Interference System to set logic that will give output as relative crack depth and relative crack location from the input as relative values of first, second and third natural frequencies. The finite element formulation was performed in ALGOR environment and the subsequent modal natural frequencies were obtained and stored in a tabular form. Figure 6.2 shows the actual view of the experimental set-up. Figure 6.3 shows the INSTRON set-up used to generate the transverse crack.

The relation between the crack depth and the first mode natural frequency is as shown in Figure 6.4. Figure 6.5 indicates the relation between the crack depth with the second mode natural frequency. And figure 6.6 shows a relation between the crack depth with the third mode



Fig. 6.2 Experimental Set-up



Figure 6.3 INSTRON Set-up

natural frequency. It was found that the natural frequency decreases gradually with increase in crack depth.

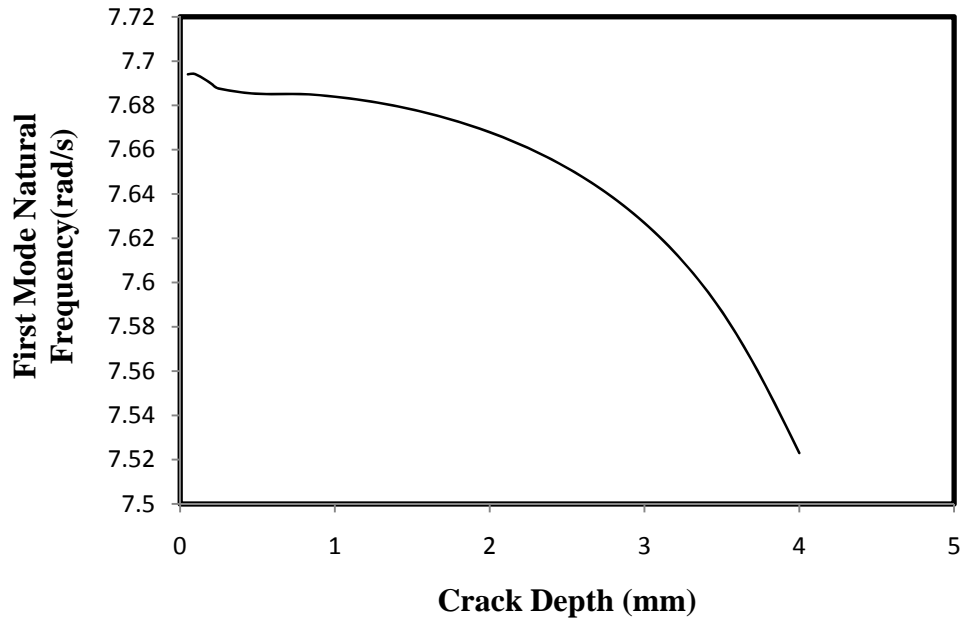


Fig. 6.4 First Mode Natural Frequency versus crack depth

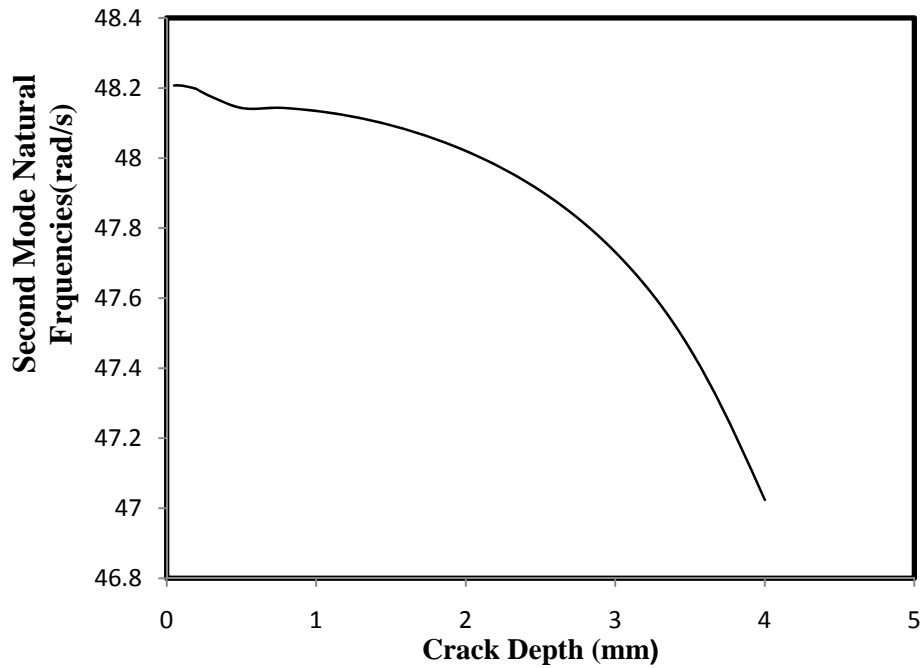


Fig. 6.5 Second Mode Natural frequency versus crack depth

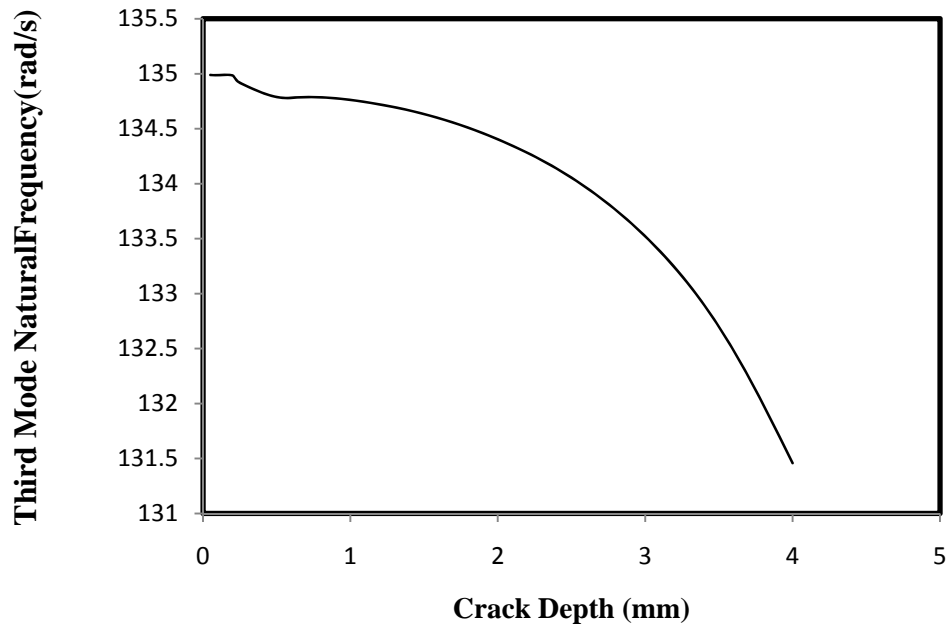


Fig. 6.6 Third mode Natural Frequency versus crack depth

The effect of crack location on the natural frequency was verified and is summarized in a graphical manner from Figure 6.7 onwards. The comparison between the first mode natural frequency at a crack length of 50 mm and 100 mm is as shown in figure 6.7. Figure 6.8 indicates the comparison between the values of the first mode of natural frequencies at 50 mm and 200 mm crack length. Figure 6.9 gives a comparative graph between the first mode natural frequencies at crack lengths of 50 mm and 300 mm. Comparative graphical representation of first mode natural frequencies between crack lengths of 50 mm and 400 mm is as shown in figure 6.10. Like-wise figures 6.11 to figure 6.13 give a comparison of first mode natural frequencies, between 50 mm and 500 mm, 50 mm and 600 mm, 50 mm and 700 mm respectively.

Figure 6.14 gives a comparison second mode of natural frequencies between crack lengths of 50 mm and 200 mm, where figure 6.15 gives the relation of third mode natural frequencies between crack lengths 50 mm and 300 mm.

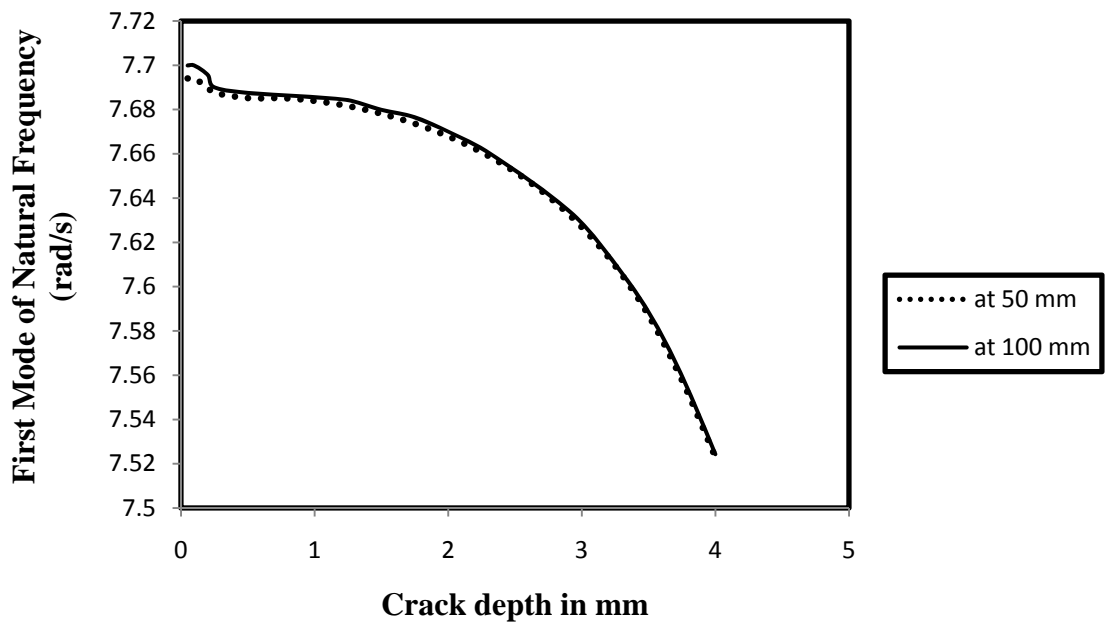


Fig. 6.7 Comparison of First Mode Natural Frequency at 50 mm and 100 mm

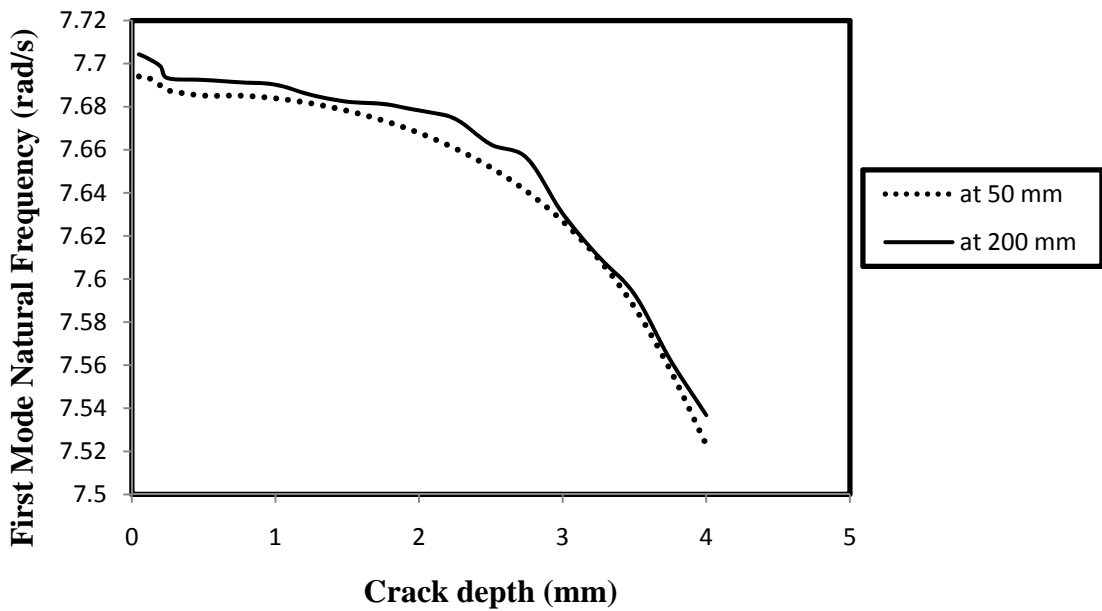


Fig. 6.8 Comparison of First Mode Natural Frequency at 50 mm and 200 mm

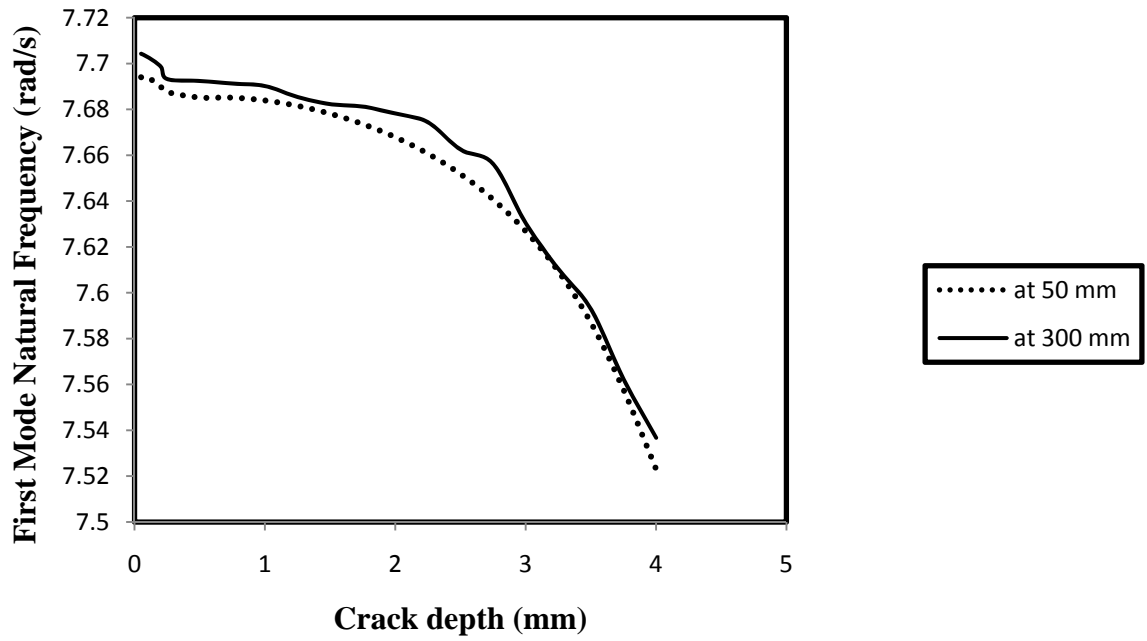


Fig. 6.9 Comparison of First Mode Natural Frequency at 50 mm and 300 mm

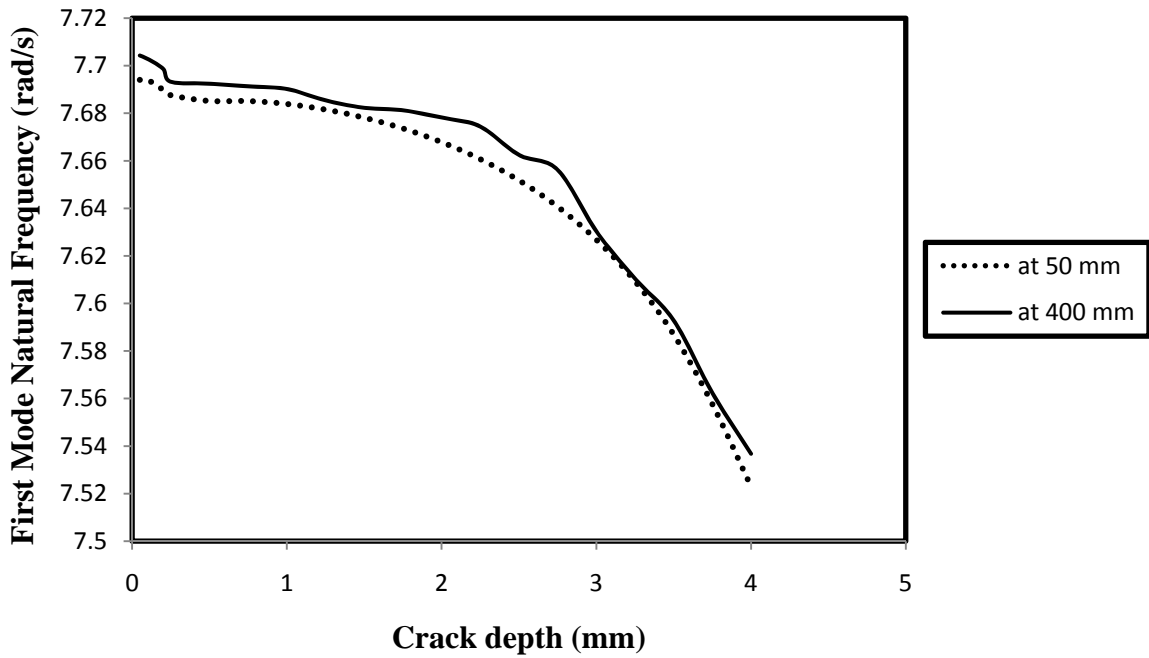


Fig. 6.10 Comparison of First Mode Natural Frequency at 50 mm and 400 mm

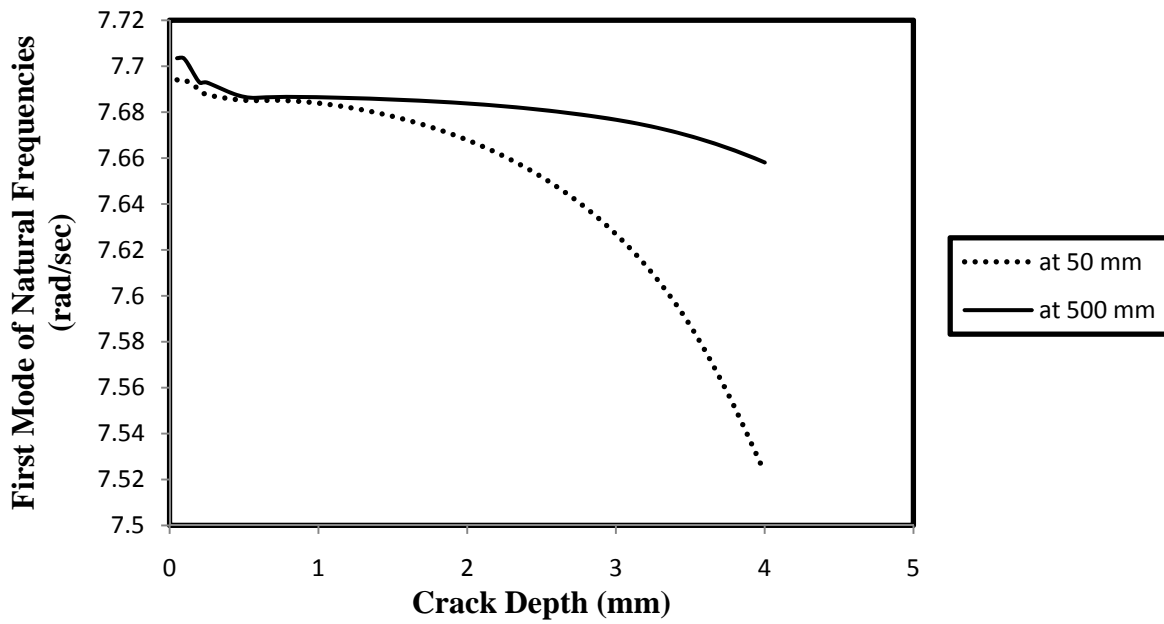


Fig. 6.11 Comparison of First Mode Natural Frequency at 50 mm and 500 mm

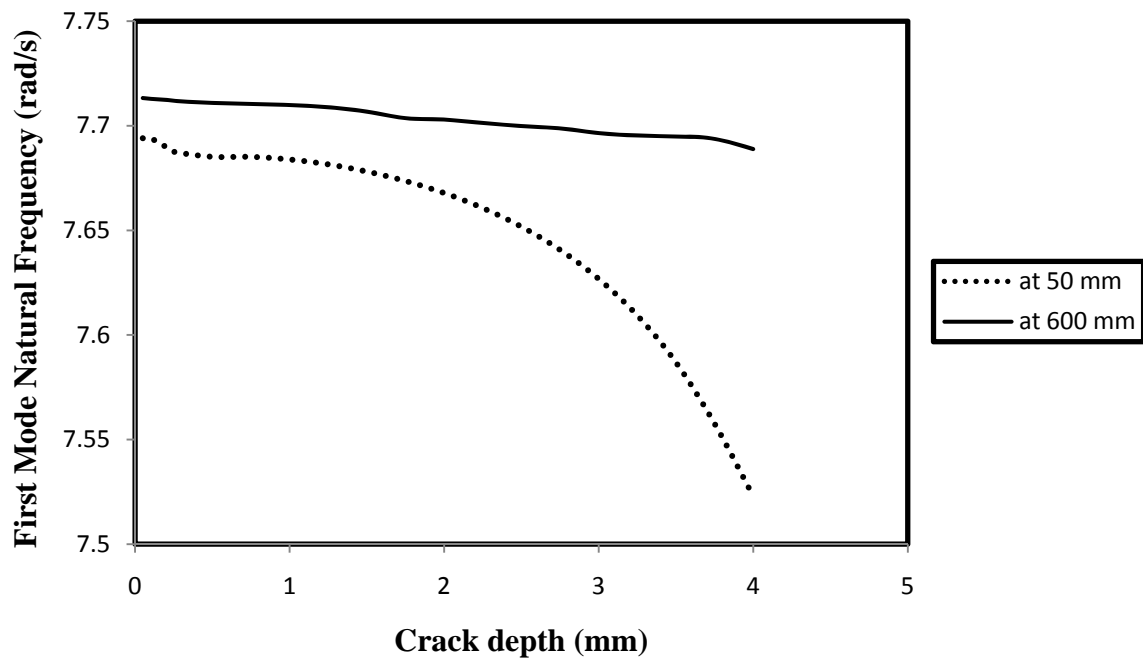


Fig. 6.12 Comparison of First Mode Natural Frequency at 50 mm and 600 mm

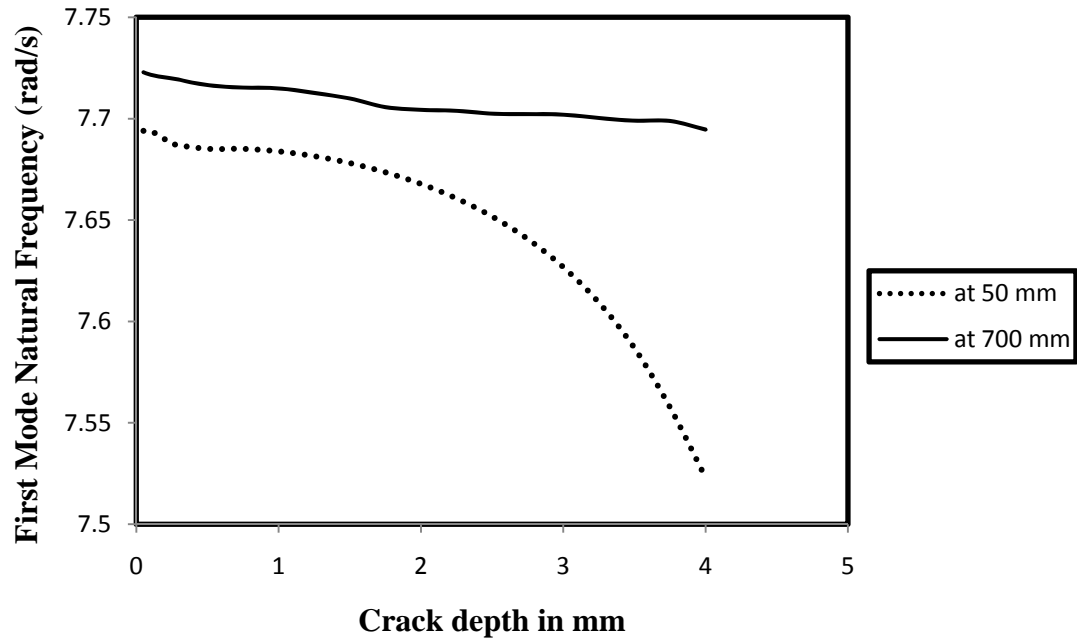


Fig. 6.13 Comparison of First Mode Natural Frequency at 50 mm and 700 mm

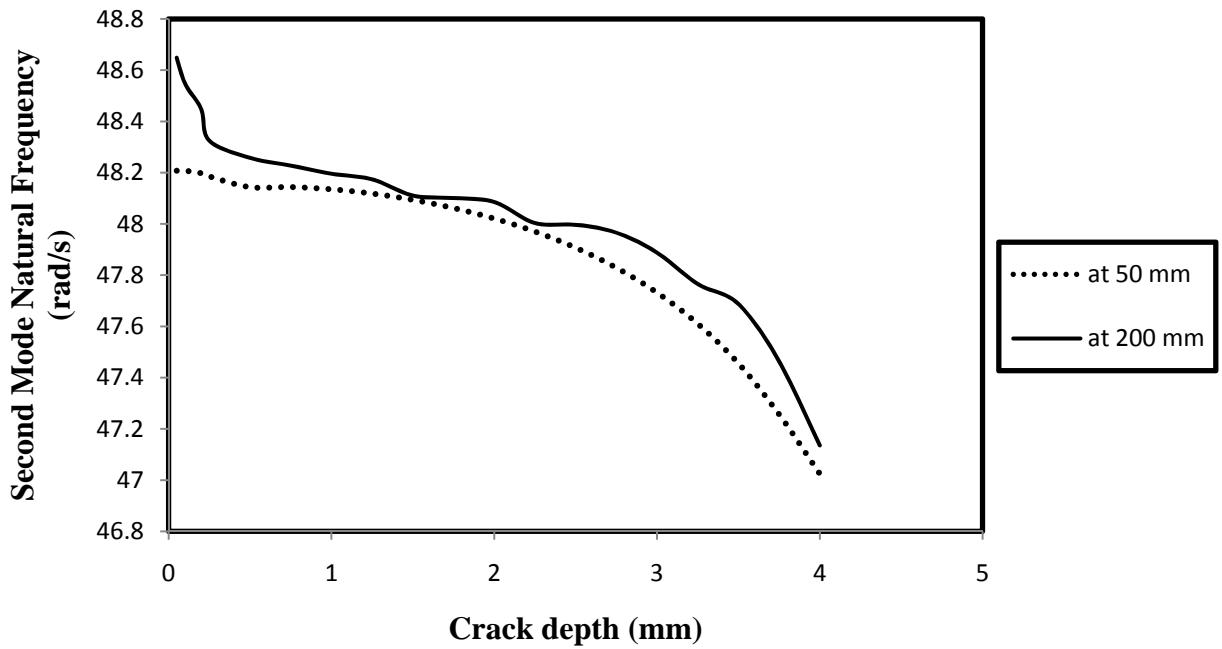


Fig. 6.14 Comparison of Second Mode Natural Frequency at 50 mm and 200 mm

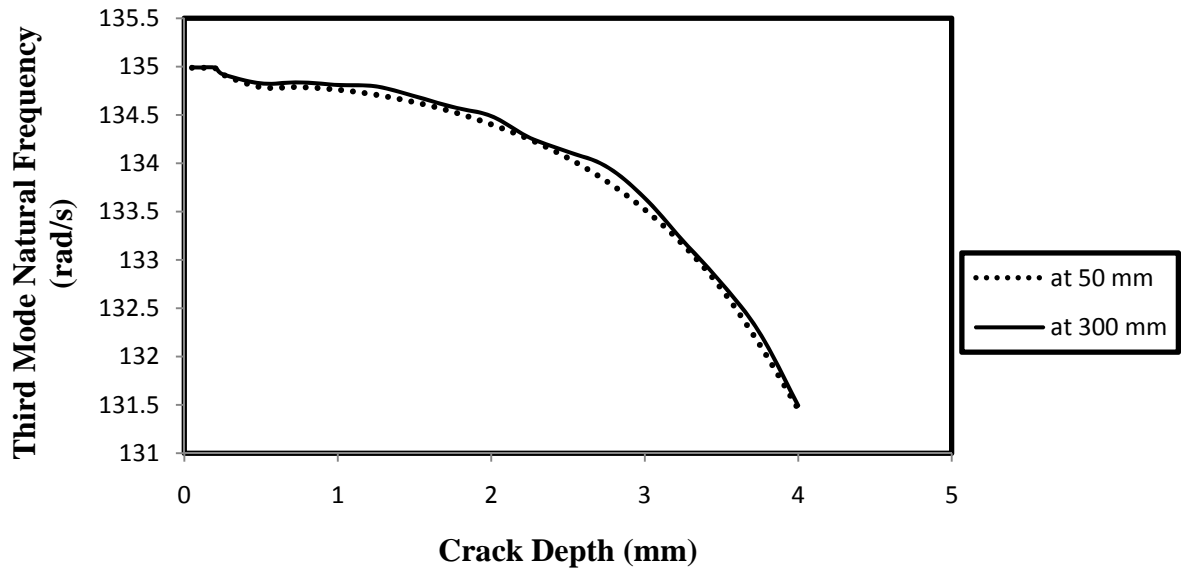


Fig. 6.15 Comparison of Third Mode Natural Frequency at 50 mm and 300 mm

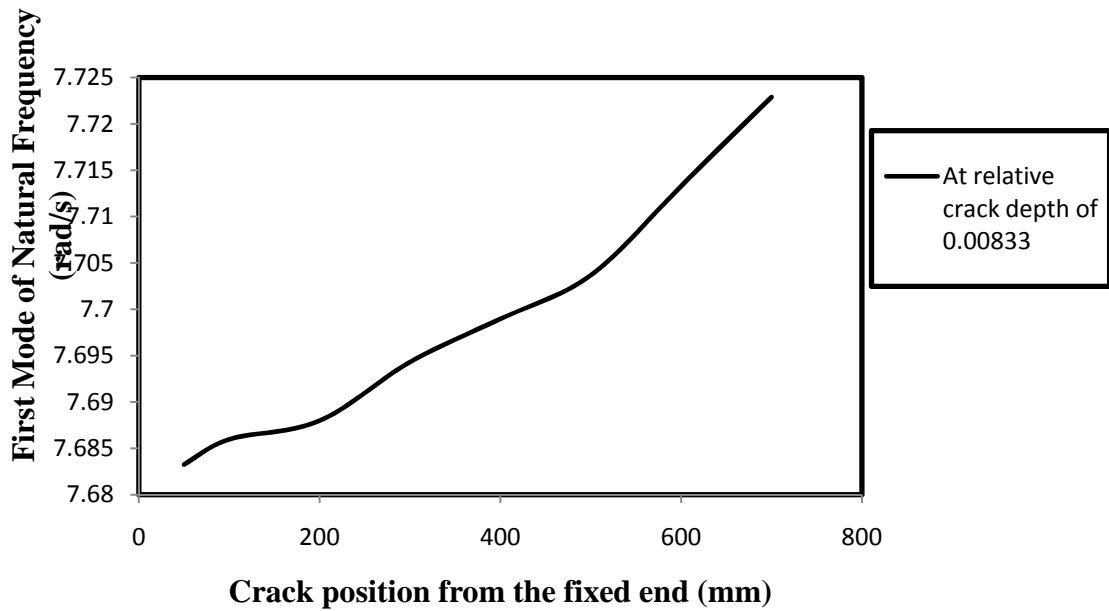


Figure 6.16 The change in First mode natural frequencies with crack location at 0.00833 relative Crack depth

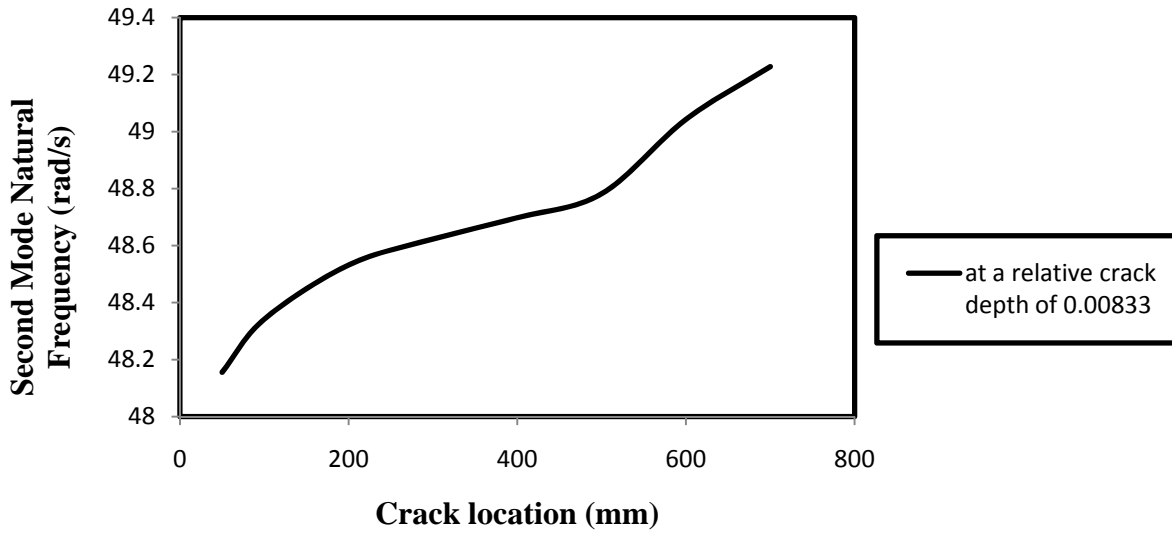


Figure 6.17 The change in Second mode natural frequencies with crack location at 0.00833 relative Crack depth

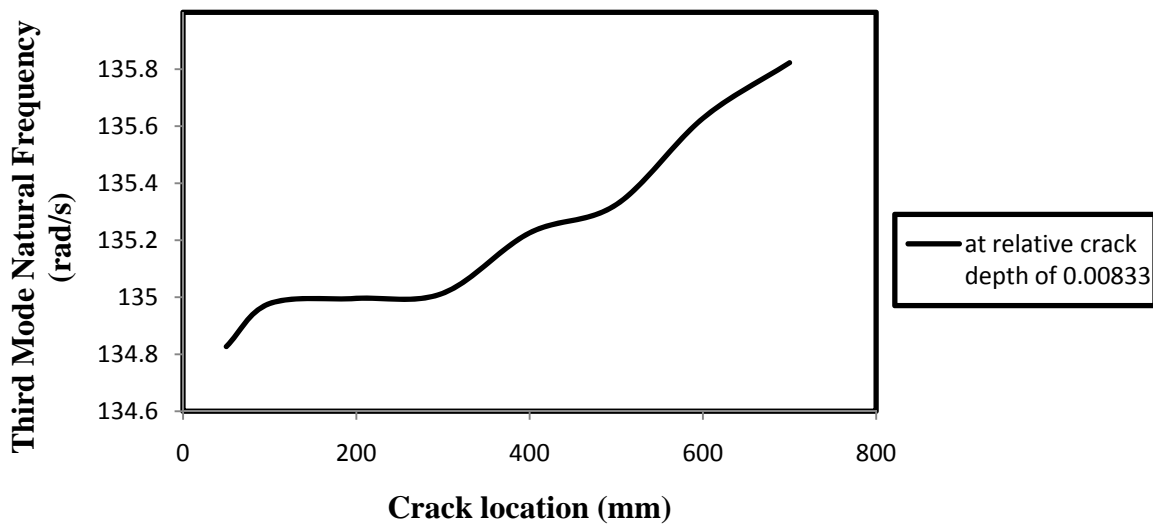


Figure 6.18 The change in Second mode natural frequencies with crack location at 0.00833 relative Crack depth

The deviation of natural frequency with respect to the crack length for the first, second and third natural frequencies are plotted as shown in figure 6.16, figure 6.17 and figure 6.18. The relative value of the crack depth is fixed at 0.00833. The comparison among the crack depth, crack length and natural frequency is as shown in the figure 6.19. First mode of natural frequency is considered in the graph. The comparison of results between the numerical analysis, fuzzy controller and the experimental analysis is as shown in a tabular format in the table 6.1.

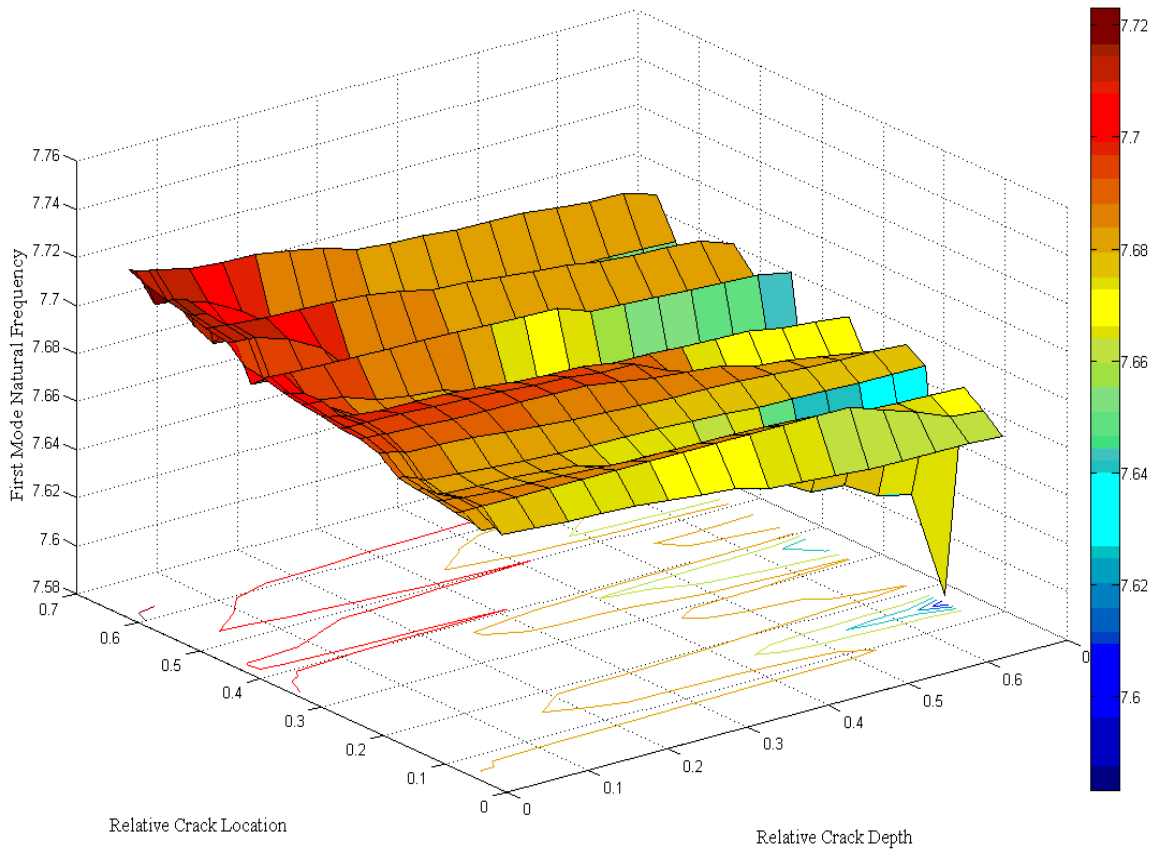
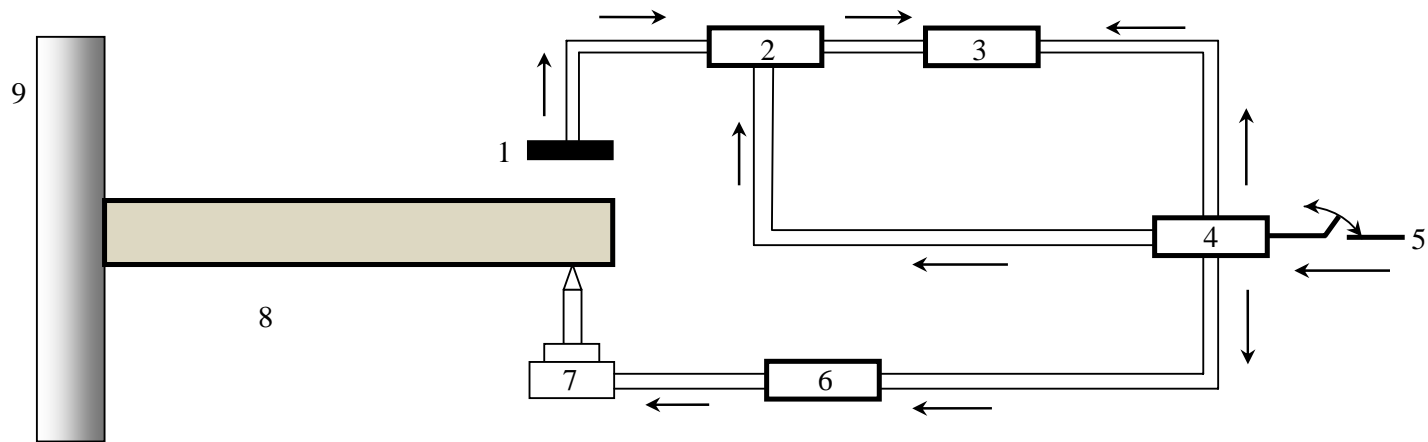


Figure 6.19 Three dimensional cum contour plot for relative First Mode Natural Frequency

6.2 Discussion

Discussions based on the outputs of the Fuzzy Controller used and the information supplemented by numerical and experimental analyses are as mentioned. The linguistic form of fuzzy rules established for the fuzzy membership functions used in the present Fuzzy Controller are given in table 4.1. Some of the sample examples of actual rules made for the Fuzzy Controller of the present investigation are enlisted in table 4.2. The present Fuzzy Controller uses Gaussian membership functions that are depicted in figure 4.1. The outputs of the Gaussian-Fuzzy Controller obtained from the activation of rule-8 and rule-20 from the table 4.2 are shown in figure 4.2. The relation between the crack depth and the three modal natural frequencies are presented in figure 6.4, figure 6.5 and figure 6.6. It was observed that the natural frequency decreases with increase in crack depth. Figure 6.7 to figure 6.18 gives the graphical presentation of the relation between the different crack location (crack positions from the fixed end) and the three modes of natural frequencies. It can be observed from the above figures that the natural frequency increases with increase in crack location from the fixed end.



- | | | |
|------------------------|---------------------|------------------------|
| 1. Vibration Pick-up | 4. Distribution Box | 7. Vibration Generator |
| 2. Amplifier | 5. Power Supply | 8. Cantilever Beam |
| 3. Vibration Indicator | 6. Power Amplifier | 9. Fixed End |

Fig. 6.1 Schematic block diagram of Experimental Set-up

Table 6.1 Comparison of Results among Fuzzy Controller, Numerical Analysis and Experimental Analysis

Relative First Natural Frequency “fnf”	Relative Second Natural Frequency “snf”	Relative Third Natural Frequency “tnf”	Fuzzy Controller Analysis (relative crack depth ‘rcd’ and crack location ‘rcf’)		Numerical Analysis (relative ‘rcd’ and crack location ‘rcf’)		Experimental Analysis (relative ‘rcd’ and crack location ‘rcf’)	
			rcd	rcf	rcd	rcf	rcd	rcf
0.9848	0.9958	0.9975	0.203	0.072	0.202	0.069	0.205	0.073
0.9673	0.9874	0.9943	0.431	0.082	0.427	0.079	0.430	0.084
0.9623	0.9948	0.9983	0.548	0.160	0.537	0.160	0.568	0.158
0.9756	0.9976	0.9972	0.389	0.188	0.394	0.187	0.391	0.188
0.9852	0.9984	0.9967	0.227	0.237	0.231	0.237	0.230	0.240
0.9723	0.9961	0.9818	0.552	0.284	0.556	0.283	0.545	0.287
0.9823	0.9872	0.9919	0.449	0.405	0.451	0.404	0.447	0.406
0.981	0.9809	0.9931	0.495	0.424	0.497	0.424	0.495	0.424
0.986	0.9842	0.9988	0.425	0.502	0.426	0.502	0.425	0.504
0.9834	0.9685	0.9974	0.537	0.534	0.542	0.535	0.535	0.534

Chapter 7

Conclusions

7. Conclusions

The present investigation based on the Fuzzy Controller, Numerical Analysis and the Experimental Analysis results draws the following conclusions.

- Theoretical analyses are performed for the single and double crack cantilever beam
- Significant changes in natural frequencies of the vibrating beam are observed at the vicinity of crack location. When the crack location is constant but the crack depth increases, the natural frequency of the beam decreases both for the single and double transverse crack in the cracked cantilever beam.
- When the crack depth is constant and crack location from the cantilever end varied for the single and double crack positions, Natural frequencies of first, second and third modes are also increased.
- The Fuzzy Controller approach has been adopted in the present investigation to predict the identification and localization of the crack with the help of modal natural frequencies in the cracked cantilever beam, found to be very efficient. The Fuzzy Controller is developed with Gaussian membership functions. The input parameters to the Fuzzy Controller are first three relative Natural Frequencies. The outputs from the Fuzzy Controller are relative crack depth and relative crack location.
- The finite element formulation is performed using the ALGOR environment and the modal natural frequencies are calculated for comparison with the values obtained in Fuzzy Controller and the Experimental Analysis.
- By Comparing the Fuzzy results with the Experimental results it is observed that the developed Fuzzy Controller can predict the relative crack depth and relative crack location in a very accurate manner.

7.1 Scope for Future Work

The proposed technique can be extended for un-symmetric crack prediction. New methodology can be adopted for robust diagnosis and condition monitoring of faulty structures.

References

- [1] Yang, J., Chen, Y., Xiang, Y., Jia, X.L, “Free and forced vibration of cracked inhomogeneous beams under an axial force and moving mass”. *Journal of Sound and Vibration*. Volume 312, (2007): pp. 166-181.
- [2] Orhan S., “Analysis of free and forced vibration of a cracked cantilever beam”. *Journal of Sound and Vibration*. Volume 40 (2007): pp. 443-450.
- [3] Taghi, M., Baghmisheh, V., Peimani, M., Sadeghi, M.H., Etefagh, M.M. “Crack detection in beam-like structures using genetic algorithms”. *Applied Soft Computing*. Volume 8 (2008): pp. 1150-1160.
- [4] Saavedra, P.N., Cuitono, L.A., “Crack detection and vibration behavior of cracked beams”. *Computers and Structures*. Volume 79 (2001): pp. 1451-1459.
- [5] Bakhary, N., Hao, H., Deeks, A.J., “Damage detection using artificial neural network with consideration of uncertainties”. *Engineering Structures*. Volume 29 (2007): pp. 2806-2815.
- [6] Friswell, M.I., Penny, J.E.T., Garvey, S.D., “A combined genetic and eigensensitivity algorithm for the location of damage in structures”. *Computers and Structures*. Volume 69 (1998): pp. 547-556.
- [7] Wang, Q., “A comprehensive stability analysis of a cracked beam subjected to follower compression”. *International Journal of Solids and Structures*. Volume 41 (2004): pp. 4875-4888.
- [8] Chondros, T.G., Dimarogonas, A.D., Yao, J., “A Continuous Cracked Beam Vibration Theory”. *Journal of Sound and Vibration*. Volume 215 (1998): pp. 17-34.
- [9] Khiem, N.T., Lien, T.V., “A Simplified Method for Natural Frequency Analysis of a Multiple Cracked Beam”. *Journal of Sound and Vibration*. Volume 245 (2001): pp. 737-751.

- [10] Cam, E., Orhan, S., Luy, M., “An analysis of cracked beam structure using impact echo method”. *NDT & E International*. Volume 38 (2005): pp. 368-373.
- [11] He-sheng, T., Song-tao, X., Rong, C., Yuan-gong, W., “Analysis on structural Damage Identification Based on Combined Parameters”. *Applied Mathematics and Mechanics*. Volume 26 (2005): pp. 44-51.
- [12] Hu, N., Fukunga, H., Kameyama, M., Mahapatra, D.R., Gopalakrishnan, S., “Analysis of Wave Propagation in Beams With Transverse and Lateral Cracks Using a Weakly Formulated Spectral Method”. *Journal of Applied Mechanics*. Volume 74 (2007): pp. 119-127.
- [13] Mei, C., Karpenko, Y., Moody, S., Allen, D., “Analytical approach to free and forced vibrations of axially loaded cracked Timoshenko beams”. *Journal of Sound and Vibration*. Volume 291 (2006): pp. 1041-1060.
- [14] Zhong, S., Oyadiji, S.O., “Analytical predictions of natural frequencies of cracked simply supported beams with a stationary roving mass”. *Journal of Sound and Vibration*. Volume 311 (2008): pp. 328-352.
- [15] Sarikdakis, K.M., Chasalevris, A.C., Papadopoulos, C.A., Dentsoras, A.S., “Applying neural networks, genetic algorithms and fuzzy logic for the identification of cracks in shafts by using coupled response measurements”. *Computers and Structures*. Volume 86 (2008): pp.1318-1338.
- [16] Li, H., He, C., Ji, J., Wang, H., Hao, C., “Crack Damage Detection in Beam-Like Structures using RBF Neural Networks with Experimental Validation”. *International Journal of Innovative Computing, Information and Control*. Volume 1 (2005): pp. 625-634.
- [17] Peng, Z.K., Lang, Z.Q., Billings, S.A., “Crack detection using nonlinear output frequency response functions”. *Journal of Sound and Vibration*. Volume 301 (2007): pp. 777-788.
- [18] Grabowska, J., Palacz, M., Krawczuk, M., “Damage identification by wavelet analysis”. *Mechanical Systems and Signal Processing*. Volume 22 (2008): pp. 1623-1635.

- [19] Law, S.S., Lu, Z.R., “Crack identification in beam from dynamic responses”. *Journal of Sound and Vibration*. Volume 285 (2005): pp. 967-987.
- [20] Pawar, P.M., Reddy, K.V., Ganguli, R., “Damage Detection in Beams using Spatial Fourier Analysis and Neural Networks”. *Journal of Intelligent Material Systems and Structures*. Volume 1 (2007): pp. 347-359.
- [21] Karthikeyan, M., Tiwari, R., Talukdar, S., “Crack localization and sizing in a beam based on the free and forced response measurements”. *Mechanical Systems and Signal Processing*. Volume 21 (2007): pp. 1362-1385.
- [22] Ostachowicz, W.M., “Damage detection of structures using spectral finite element method”. *Computers and Structures*. Volume 86 (2008): pp. 454-462.
- [23] Das, H.C., Parhi, D.R., “Detection of the Crack in Cantilever Structures Using Fuzzy Gaussian Inference Technique”. *AIAA Journal*. Volume 47 (2009): pp. 105-125.
- [24] Nahvi, H., Jabbari, M., “Crack detection in beams using experimental modal data and finite element model”. *International Journal of Mechanical Science*. Volume 47 (2005): pp. 1477-1497.
- [25] Loutridis, S., Douka, E., Trochidis, A., “Crack identification in double-cracked beams using wavelet analysis”. *Journal of Sound and Vibration*. Volume 277 (2004): pp. 1025-1039.
- [26] Wang, K., Inman, D.J., Farrar, C.R., “Crack-induced Changes in Divergence and Flutter of Cantilevered Composite Panels”. *Structural Health Monitoring*. Volume 4 (2005): pp. 377-392.
- [27] Maity, D., Saha, A., “Damage assessment in structure from changes in static parameter using neural networks”. *Sadhana*. Volume 29 (2004): pp. 315-327.
- [28] Hwang, H.Y., Kim, C., “Damage detection in structures using a few frequency response measurements”. *Journal of Sound and Vibration*. Volume 270 (2004): pp. 1-14.

- [29] Patil, D.P., Maity, S.K., “Detection of multiple cracks using frequency measurements”. *Engineering Fracture Mechanics*. Volume 70 (2003): pp. 1553-1572.
- [30] Chang, C.C., Chen, L.W., “Detection of the location and size of cracks in the multiple cracked beam by spatial wavelet based approach”. *Mechanical Systems and Signal processing*. Volume 19 (2005): pp. 139-155.
- [31] Viola, E., Federici, L., Nobile, L., “Detection of crack location using cracked beam element method for structural analysis”. *Theoretical and Applied Fracture Mechanics*. Volume 36 (2001): pp. 23-35.
- [32] Li, J., Hua, H., Shen, R., “Dynamic Stiffness Analysis of a Beam Based on Trigonometric Shear Deformation Theory”. *Journal of Vibration and Acoustic*. Volume 130 (2008): pp. 1-7.
- [33] Han, S.M., Benaroya, H., Wei, T., “Dynamics of Transversely Vibrating Beams using Four Engineering Theories”. Volume 225 (1999): pp. 935-988.
- [34] Xu, G.Y., Zhu, W.D., Emory, B.H., “Experimental and Numerical Investigation of Structural Damage Detection Using Changes in Natural Frequencies”. Volume 129 (2007): pp. 686-700.
- [35] Qiao, P., Cao, M., “Waveform fractal dimension for mode shape-based damage identification of beam-type structures”. *International Journal of Solids and Structures*. Volume 45 (2008): pp. 5946-5961.
- [36] Duffey, T.A., Doebling, S.W., Farrar, C.R., Baker, W.E., Rhee, W.H., “Vibration-Based Damage Identification in Structures Exhibiting Axial and Torsional Response”. *Journal of Vibration and Acoustic*. Volume 123 (2001): pp. 84-91.
- [37] Dimarogonas, A., “Vibration of Cracked Structures: A State of the Art Review”. *Engineering Fracture Mechanics*. Volume 55 (1996): pp. 831-857.
- [38] Binici, B., “Vibration of beams with multiple open cracks subjected to axial force”. *Journal of Sound and Vibration*. Volume 287 (2005): pp. 277-295.

- [39] Chondros, T.G., Dimarogonas, A.D., “Vibration of a Cracked Cantilever Beam”. *Journal of Vibration and Acoustic*. Volume 120 (1998): pp. 742-746.
- [40] Shih, H.W., Thambiratnam, D.P., Chan, T.H.T., “Vibration based structural damage detection in flexural members using multi-criteria approach”. *Journal of Sound and Vibration*. Volume 328 (2007): 127-144.
- [41] Mazanoglu, K., Yesilyurt, I., Sabuncu, M., “Vibration analysis of multiple-cracked non-uniform beams”. *Journal of Sound and Vibration*. Volume 320 (2009): pp. 977-989.
- [42] McAdams, D.A., Tumer, I.Y., “Toward Intelligent Fault Detection in Turbine Blades: Variational Vibration Models of Damaged Pinned-Pinned Beams”. *Journal of Vibration and Acoustic*. Volume 127 (2005): pp. 467-474.
- [43] Escobar, J.A., Sosa, J.J., Gomez, R., “Structural damage detection using the transformation matrix”. *Computers and Structures*. Volume 83 (2005): pp. 357-368.
- [44] Fang, X., Luo, H., Tang, J., “Structural damage detection using neural network with learning rate improvement”. *Computers and Structures*. Volume 83 (2005): pp. 2150-2161.
- [45] Sekhar, A.S., “Multiple cracks effects and identification”. *Mechanical Systems and Signal Processing*. Volume 22 (2008): pp. 845-878.
- [46] Hearndon, J.L., Potirniche, G.P., Parker, D., Cuevas, P.M., Rinehart, H., Wang, P.T., Horstemeyer, M.F., “Monitoring structural damage of components using an effective modulus approach”. *Theoretical and Applied Fractural Mechanics*. Volume 50 (2008): pp. 23-29.
- [47] Lee, J., “Identification of multiple cracks in a beam using natural frequencies”. *Journal of Sound and Vibration*. Volume 320 (2009): pp. 482-490.
- [48] Park, J., “Identification of damage in beam structures using flexural wave propagation characteristics”. *Journal of Sound and Vibration*. Volume 318 (2008): pp. 820-829.

- [49] Tada, H., Paris P.C., Irwin, G.R., “The Stress Analysis of Cracks Handbook”. Del Research Corporation. Hellertown, Pennsylvania, U.S.A., 1985
- [50] Yen, J., Langari, R., “Fuzzy Logic Intelligence Control and Information”. Pearson Education. 1999
- [51] ALGOR Release V 19.3 SP-2, 2007, <http://nitrkl.ac.in/intranet/softwarevault>